Physics – Uspekhi **65** (1) 40 – 61 (2022)

REVIEWS OF TOPICAL PROBLEMS

PACS numbers: 42.25.Fx, **42.70. – a**, **78.67. – n**

Resonant scattering of electromagnetic waves by small metal particles: a new insight into the old problem

M I Tribelsky, A E Miroshnichenko

DOI: https://doi.org/10.3367/UFNe.2021.01.038924

Contents

Abstract. This review is devoted to a discussion of new (and often unexpected) aspects of the old problem of elastic light scattering by small metal particles, whose size is comparable to or smaller than the thickness of the skin layer. The main focus is on elucidating the physical grounds for these new aspects. It is shown that, in many practically important cases, the scattering of light by such particles, despite their smallness, may have almost nothing in common with the Rayleigh scattering. So-called anomalous scattering and absorption, as well as Fano resonances, including unconventional (associated with the excitation of longitudinal electromagnetic oscillations) and directional Fano resonances, observed only at a small solid angle, are discussed in detail. The review contains a Mathematical Supplement, which includes a summary of the main results of the Mie theory and a discussion of some general properties of scattering coefficients. In addition to being of purely academic interest, the phenomena considered in this review can find wide applications in biology, medicine, pharmacology, genetic engineering, imaging of ultra-small objects, ultra-high-resolution spectroscopy, information transmission, recording, and processing, as well as many other applications and technologies.

M I Tribelsky [1,2,a], **A E Miroshnichenko** [3]
[1] Lomonosov Moscow State University, Faculty of Physics, Leninskie gory 1, str. 2, 119991 Moscow, Russian Federation
[2] National Engineering Physics Institute MEPhI, Engineering and Physics Institute of Biomedicine, Kashirskoe shosse 31, 115409 Moscow, Russian Federation
[3] School of Engineering and Information Technology, University of New South Wales (UNSW), Canberra, Australia
E-mail: [a] mitribel@gmail.com

Received 17 August 2020, revised 22 January 2021
Uspekhi Fizicheskikh Nauk **192** (1) 45 – 68 (2022)
Translated by M I Tribelsky, A E Miroshnichenko

Keywords: Mie resonances, Fano resonances, subwavelength optics, nanoparticles

1. Introduction

Light scattering by small particles has a long history. However, even though the exact solution for a spatially uniform spherical particle of an arbitrary size, which has an arbitrary permittivity value, was obtained by Gustav Mie (and independently by Lorentz and Debye) more than 100 years ago, [1] it is not entirely understood yet. The point is that, in the Mie solution, the scattered wave field is presented in the form of an infinite series of partial waves (dipole, quadrupole, etc.). Each of them, in turn, is divided into the sum of the so-called electric and magnetic components [1–4]. The corresponding efficiencies (dimensionless values, equal to the ratio of partial cross-sections to the geometric section area of the sphere, πR^2) are expressed in terms of the scattering coefficients a_n, b_n by quite simple formulas (see below).

However, the devil is in the details: explicit expressions for the scattering coefficients themselves are cumbersome combinations of special functions (so-called Riccati–Bessel functions); see the Appendix (Mathematical supplement) to this review. Their dependence on the problem's parameters varies dramatically in different characteristic domains of the values of these parameters. This, in turn, leads to a qualitative difference in the scattering properties in various regions of the parameter space. In contrast to the formal mathematical Mie solution, splitting the parameter space into these domains and elucidating the scattering properties in each domain are physical problems. Just these problems have not

[1] An excellent historical overview of this problem is contained in Kerker's book [1].

been completely solved yet and still presents unexpected and significant results to the curious researcher.

Recently, interest in it has increased drastically, mainly due to the enormous progress in nanotechnology and, as a result, the broad application of the results of the Mie theory and its generalizations in a wide variety of fields ranging from telecommunications to diagnosing and treating oncological and other diseases [5–9]. Accordingly, it has increased the number of publications on this topic. A search using *Google Scholar* with the keywords *Mie scattering* yields 213,000 (!) monographs, articles, and software products.

Of course, there is no way to present an overview of this entire mass of material in a single manuscript. The authors of this review do not lay before themselves such an impossible task. Fortunately, there are already a large number of both excellent monographs (see, for example, [1, 3, 4]) and remarkable reviews [10–15] devoted to this topic. However, since progress in this field is accelerating, even the most recent reviews become obsolete by the time they are published. For this reason, we decided to concentrate only on those recent achievements in this area which are closest to the authors' own research. Alas, even here, we do not claim completeness, limiting ourselves to a few of what, from our point of view, are the most interesting issues of scattering and absorption of electromagnetic radiation by small metal particles, leaving the discussion of dielectric particles for a future review, if one is ever written. At the same time, we did our best to focus on the physics of the discussed phenomena, limiting ourselves to a minimum number of simple formulas.

Regarding cumbersome mathematical expressions, inevitable in scattering theory, they are all moved to the Appendix. We will also disregard the anisotropy of a particle, believing that all three principal values of the dielectric constant tensor of the particle material are equal. Considering the anisotropy, unless we are talking about specially fabricated nanoparticles with large anisotropy, would be an excess of the accepted accuracy of the consideration. The discussion of experiments is also limited to the most necessary minimum.

However, when, following these principles, we started writing this review, it turned out that even these limitations were still insufficient to keep the size of the review within reasonable limits. Therefore, they had to be tightened. In particular, the problems of the optical properties of metamaterials (artificial, specially structured media) and 'metamolecules' — several nanoparticles separated by gaps smaller than or comparable to the wavelength of the incident radiation — had to be excluded from the review. Readers interested in these issues should turn to other original and review literature; see, for example, [16–20]. What is left after all the constraints were set is effects arising from the scattering of light by a spatially uniform spherical metal particle or a spherically symmetric core-shell particle, which will be discussed in sufficient detail.

Since different readers may have different areas of interest, we have tried to ensure that every section of the review can stand alone, while maintaining the unity of the presentation and its logical consistency. This makes it possible, if desired, to limit reading to only individual sections of the review.

Wherever this is not explicitly stated, we will consider the scattering of a linearly polarized plane wave with the time dependence $\exp(-i\omega t)$. Since plane waves form a complete set of functions, and hence an arbitrary incident wave can be presented as their superposition, such a consideration does not limit the generality of the results discussed.

We will use the Gaussian system of units. In addition, all substances are assumed to be nonmagnetic, so that the magnetic permeability μ is always considered equal to unity. Only passive scattering is discussed. Scattering by active particles with an inverse population and the associated laser effects lie outside the scope of this paper. We emphasize that, although everywhere in this review we talk about the scattering of electromagnetic waves, the given results are readily transferred to cases of scattering of waves of a different nature, for example, acoustic.

2. Plasmonic resonances

2.1 Rayleigh scattering and its range of applicability

The fact that a subwavelength particle scatters electromagnetic radiation as an electric dipole has been well known since the fundamental work by Lord Rayleigh [21, 22], published 150 years ago! We are convinced of the accuracy of these studies every time we admire the blue sky or a crimson sunset. Later, their results were brilliantly confirmed by countless experimental and theoretical researches. It would seem that the issue has been resolved once and for all, and nothing new can ever be discovered here.

But, never say never. Let us briefly replicate and analyze the reasoning behind the famous formula for the Rayleigh scattering cross-section for a spherical particle of radius R immersed in a transparent medium* [23]:

$$\sigma_{\rm sca} = \frac{8\pi\varepsilon_{\rm out}^2}{3}\left(\frac{\omega}{c}\right)^4 R^6\left|\frac{\varepsilon-1}{\varepsilon+2}\right|^2 \equiv \frac{8\pi x^6}{3k^2}\left|\frac{\varepsilon-1}{\varepsilon+2}\right|^2. \qquad (1)$$

Here, $\varepsilon \equiv \varepsilon_1/\varepsilon_{\rm out}$ stands for the dielectric constant of the particle material ε_1, normalized by the corresponding value for the ambient medium $\varepsilon_{\rm out}$, and the value of x (size parameter) is equal to kR, where $k = \omega m_{\rm out}/c$ is the wavenumber of the incident wave, $m_{\rm out} \equiv \sqrt{\varepsilon_{\rm out}}$ designates the refractive index of the ambient medium, and c is the speed of light in a vacuum. Owing to the transparency of the ambient medium, $m_{\rm out}$ and hence x are both purely real quantities. It is relevant to mention that the employed problem formulation (unbounded space; the incident wave comes from infinity and the scattered radiation goes to infinity too) is only possible with a purely real value of $m_{\rm out}$. Note that, often, along with the dimensional quantity $\sigma_{\rm sca}$, it is convenient to characterize the scattering intensity by the mentioned above dimensionless scattering efficiency: $Q_{\rm sca} = \sigma_{\rm sca}/(\pi R^2)$.

Suppose the shape of the light scattering particle is close to spherical, and its radius is significantly less than the radiation wavelength, including its value in the particle's material. In this case, in the particle and its proximity at any given moment of time, the electric field of the incident wave may be regarded as spatially uniform. Then, as follows from the problem symmetry, the total field inside the particle (i.e., the sum of the external one and the field caused by the particle's polarization) is also spatially uniform. However, naturally, the value of the vector $\mathbf{E}$ inside the particle is determined by ε and is different from the corresponding value in the incident wave [23]. A uniform field creates an induced dipole moment in the particle, whose value is proportional to the volume of the particle, i.e., R^3, and oscillates in time with incident wave

* The ambient medium and particle are both regarded as homogeneous and isotropic. (*Authors' note to English proof.*)

circular frequency ω. Regarding the magnetic polarizability, at μ close to one, it can be ignored. The intensity of electric dipole radiation is proportional to the square of the modulus of the second derivative in time from the value of the dipole moment [24], i.e., $\omega^4 R^6$. These arguments are the physical grounds for the dependence $\sigma(\omega, R)$ following from Eqn (1).

What is not taken into account in this reasoning? In addition to $\omega^4 R^6$, Eqn (1) has the multiplier $|(\varepsilon - 1)/(\varepsilon + 2)|^2$, which describes the polarizability of a particle by a spatially uniform electric field [23]. Note now that, for good metals in the optical range of the spectrum, $\varepsilon < 0$, and the denominator in Eqn (1) vanishes at $\varepsilon = -2$. We arrive at the nonphysical result of divergence of the scattering cross-section. To avoid any misunderstanding, note that, although at $\varepsilon < 0$ the field in the metal exponentially decays, this does not contradict our assumption that there is a spatially uniform field inside the scattering particle: as noted above, the particle size is regarded as much smaller than the characteristic length of the field decay (skin layer depth).

The argument that a purely real ε corresponds to an idealized nondissipative case, that any actually existing material always possesses some dissipation, and hence ε always has a nonzero imaginary part describing the dissipation, does not save the day. Indeed, if ε has a nonzero imaginary part, the denominator in Eqn (1) cannot be set to zero. However, there are no fundamental limitations from below on the value of $\operatorname{Im}\varepsilon$, except that it must be positive to ensure dissipation. Owing to the principle of causality, it must satisfy the Kramers–Kronig relation, which is a certain *integral* identity. As for the value of $\operatorname{Im}\varepsilon$ at some fixed frequency ω, there may be cases when it is extremely small. If at ω corresponding to this extremely small value of $\operatorname{Im}\varepsilon$ simultaneously $\operatorname{Re}\varepsilon \approx -2$, then it may be that, according to Eqn (1), a particle with a radius of several nanometers has a scattering cross-section of about a square kilometer. This, obviously, cannot be the case, since it contradicts elementary common sense. Speaking of a square kilometer, we, of course, exaggerate, but it is clear that in the vicinity of $\varepsilon = -2$ the Rayleigh approximation may lead to absurd results, i.e., it stops working, and expression (1) requires some modifications.

Let us approach this important issue from another side. Microscopically, the dipole moment oscillations are associated with collective oscillations of free and/or bound charges in the substance of the scattering particle. These oscillations have their own eigenfrequencies. In the absence of dissipation, when the drive frequency becomes equal to the eigenfrequency of the oscillations, their amplitude diverges. Obviously, the discussed divergence of expression (1) at $\varepsilon = -2$ just means such a resonant excitation. This is highly consistent with a fact known in scattering theory: the divergence of the elastic scattering cross-section at the resonance points [25].

Since, as already noted, negative values of ε in the visible region of the spectrum usually correspond to metals, we will, for certainty, talk about free electrons. The electron plasma oscillations noted above are called localized plasmons. Thus, when a small metal particle scatters light, energy is pumped from the incident electromagnetic wave to the localized plasmons. However, in the absence of dissipation, all processes are reversible. If there is a direct process, then there must also be an inverse one, namely transformation of the localized plasmons into a scattered electromagnetic wave getting out of the particle.

This process is well known and is called radiative damping of the plasmon. In this case, if the amplitude of the incident wave determines the energy flow in the direct process, then, in the inverse process, it is determined by the amplitude of the plasmon. Usually, the radiative damping is very small; see below. Nevertheless, it is clear that, no matter how small the efficiency of the inverse process is, with an unbounded increase in plasmon amplitude eventually, this amplitude reaches such a value when both processes (direct and inverse) come into dynamic equilibrium. Then, a further increase in the plasmon amplitude, and hence the scattered radiation power, is terminated. It is essential that, due to the weakness of the radiative damping, the localized plasmon has a long lifetime.

Suppose, at some point in time, a sudden jump switches off the incident radiation. In this case, the energy stored in the localized plasmon will not radiate instantly but will decrease gradually according to an exponential law with a decrement equal to the inverse lifetime of the plasmon. Therefore, at dynamic equilibrium, the energy flux during the direct transformation of the incident electromagnetic wave into localized plasmons is compensated by the opposite flux of the radiative damping of the plasmons excited *at previous moments of time*. In other words, there is a certain retardation between direct and inverse transformations.

It now becomes clear what Eqn (1) does not describe. This equation is based on the consideration of the particle's polarization by a stationary electric field. Such a description, in principle, cannot include retardation effects, i.e., radiative damping. Far from the plasmon resonance, this damping can indeed be disregarded owing to its smallness, which leads to Eqn (1). However, in the case of small dissipation, in the vicinity of the resonance, this disregard becomes unacceptable, since exactly radiative damping bounds the scattering cross-section.

2.2 Anomalous scattering

2.2.1 Lossless limit. What do we need to do to take into account the radiative damping accurately? Surprisingly, very little. We have the exact solution to the problem [1–3]; see also the Appendix. Since it is exact, the radiative damping is automatically included in this solution. The only thing to be done is to single out the effects of the radiative damping in an explicit form. To this end, we have to simplify the cumbersome Mie formulas, taking advantage of the small x.

To begin with, consider a lossless limit ($\operatorname{Im}\varepsilon = 0$). Of course, such a limit is an idealization and never occurs in nature. However, it is of particular interest because, first, it most clearly demonstrates the new effects discussed below. Second, with small dissipation (the specific criteria for the smallness will be formulated below), these effects for the lossless and lossy cases are close not only qualitatively but also quantitatively. As for their analysis, in the nondissipative case, it is significantly simplified, which makes it especially important for understanding the essence of the discussed phenomena.

Let us recall the main results of Mie's theory; see also the Appendix. In this theory, the scattered wave field is presented as a multipole expansion, i.e., as an infinite series of spherical harmonics (dipole, quadrupole, octupole, etc.). Every harmonic, in turn, is a sum of two independent components, electric and magnetic, which we will call electric and magnetic partial modes. It is customary to denote the complex amplitudes of the first and second components (*scattering coefficients*) as a_n and b_n, respectively, where $n = 1, 2, 3, \ldots$ stands for the multipole number.

The values of the scattering coefficients are determined from the boundary conditions stipulating the continuity of the tangential components of fields **E** and **H** on the surface of the particle. Note that, due to the linearity of the problem, the general solutions to Maxwell's equations describing the fields within the particle and outside it do not depend on each other. From this relatively trivial statement, an important conclusion follows: namely, the functional form of the solution to the outer problem does not depend on the coordinate dependence of $\varepsilon(r)$ inside the particle, provided it does not violate the problem's symmetry (this statement, of course, is valid in the cylindrically-symmetric case too). A specific type $\varepsilon(r)$ defines only the values of the scattering coefficients, but not the structure of the solution itself.

As shown below, this makes it possible to arrive at certain very general conclusions about the properties of the scattering problem for a sphere with an arbitrary (including a discontinuous — layered structure) dependence of its permittivity on radius. This opportunity is especially significant due to the complexity of the dependence of the scattering coefficients on the parameters of the problem, which, even in the simplest case of a spatially homogeneous sphere, is expressed in terms of Riccati–Bessel functions and is cumbersome; see the Appendix. In particular, it can be shown ([26]; see also the Appendix) that, from the general properties of the exact solution, it follows that for a sphere with an arbitrary dependence $\varepsilon(r)$, including discontinuous — a layered structure,

$$a_n = \frac{F_n^{(a)}}{F_n^{(a)} + \mathrm{i}G_n^{(a)}}\,, \tag{2}$$

where the specific expressions of F and G are governed by $\varepsilon(r)$ and the size parameter x. A similar expression is valid for b_n, of course, with different values of F and G than those for a_n.

Regarding the scattering cross-section, according to the definition, it is equal to the ratio of the energy flux scattered in all directions to the intensity of the incident wave [1–4]. To calculate this flux, it is convenient to take the flux of the Poynting vector through a spherical surface located in the far wave zone, the center of which coincides with the one for the scattering particle. During the integration over the surface of such a sphere, cross terms corresponding to the products of fields of different partial modes vanish owing to the orthogonality of the spherical harmonics. As a result, the scattering intensity in each partial mode is independent of the others. Then, the entire scattering cross-section is presented as an infinite series of partial cross-sections $\sigma_{n,\,\mathrm{sca}}$, while each of these is associated with scattering coefficients by the following relations [1, 3, 27]:

$$\sigma_{n,\,\mathrm{sca}} = \sigma_{n,\,\mathrm{sca}}^{(a)} + \sigma_{n,\,\mathrm{sca}}^{(b)}\,, \quad \sigma_{n,\,\mathrm{sca}}^{(z)} = \frac{2(2n+1)\pi}{k^2}\,|z_n|^2\,, \tag{3}$$

where z denotes either a or b.

In the nondissipative case ($\operatorname{Im}\varepsilon = 0$), the functions F and G are purely real. Next, unless this is not specifically stated, we will limit ourselves to the consideration of a spatially homogeneous sphere, for which $\varepsilon = \mathrm{const}$. In this case, expanding the functions F and G (whose explicit form is given in the Appendix) in series in small x, it is easy to make sure that, at $|mx| \ll 1$, where $m \equiv \sqrt{\varepsilon}$, the expression for b_n does not have a resonant denominator, and b_n itself is of the order of x^{2n+3}. Regarding a_n, keeping just the leading terms in the expansion of the numerator and denominator of expression (2) and canceling their common factor, we get

$$F_n^{(a)} = x^{2n+1}\left\{\frac{(n+1)(\varepsilon-1)}{\left[(2n+1)!!\right]^2} + O(x^2)\right\}, \tag{4}$$

$$G_n^{(a)} = \frac{n}{2n+1}\left(\varepsilon + \frac{n+1}{n} + O(x^2)\right). \tag{5}$$

It would seem that, since F_n is of the order of x^{2n+1}, and the leading term in the expansion of G_n in powers of x does not depend on x at all, either we can always ignore F_n relative to G_n in the denominator of Eqn (2), or it is necessary to consider on the r.h.s. of Eqn (5) terms up to x^{2n+1} inclusively. However, because function G_n enters into expression (2), with the multiplier i, this question turns out to be somewhat more subtle. Let us take a closer look at it.

If $(\varepsilon + 1 + 1/n) \gg x^{2n+1}$, then F in the denominator of Eqn (2) indeed may be disregarded relative to G. In this case, all a_n become purely imaginary quantities, and $|a_n|$ turns out to be of the order of x^{2n+1}. The substitution of the corresponding expressions in Eqn (3) gives the value of the scattering partial cross-section, which may be regarded as a generalization of formula (1) to the case of an arbitrary n. In particular, at $n = 1$, we get exactly Eqn (1). With an arbitrary n, the corresponding partial cross-section is of the order of $x^{2(2n+1)}$. This circumstance, together with the noted smallness of b_n relative to a_n, leads to the fact that the electric dipole moment makes the overwhelming contribution to the entire infinite series of the multipole expansion, in full accordance with the above discussion of formula (1).

Here, it is appropriate to make a certain general comment regarding the minimal required accuracy of approximate calculations for the problem in question. In addition to σ_{sca}, an important parameter describing the scattering process is the extinction cross-section $\sigma_{\mathrm{ext}} \equiv \sigma_{\mathrm{sca}} + \sigma_{\mathrm{abs}}$, where σ_{abs} is the absorption cross-section characterizing the power absorbed by the radiation scattering object due to irreversible dissipative processes. For a spherical particle, the extinction partial cross-section is defined by the following formula [1, 3, 27]:

$$\sigma_{n,\,\mathrm{ext}} = \sigma_{n,\,\mathrm{ext}}^{(a)} + \sigma_{n,\,\mathrm{ext}}^{(b)}\,, \quad \sigma_{n,\,\mathrm{ext}}^{(z)} = \frac{2(2n+1)\pi}{k^2}\,\operatorname{Re} z_n\,, \tag{6}$$

where, as before, z_n denotes any of the coefficients a_n, b_n.

In the nondisipative limit, $\sigma_{\mathrm{abs}} = 0$, and therefore $\sigma_{\mathrm{ext}} = \sigma_{\mathrm{sca}}$. However, if, in accordance with the above, we limit the accuracy of expression (2) to the leading approximation in small F, the real part of the resulting purely imaginary quantity is zero, while its modulus, obviously, is not. Then, the equality $\sigma_{\mathrm{ext}} = \sigma_{\mathrm{sca}}$ does not hold. The paradox is easily resolved, given that, in approximate calculations, the vanishing of the leading term means only that the next term of the corresponding expansion must be taken into account. In Eqn (3) for the scattering partial cross-section, the leading term is not equal to zero, and higher-order terms may be discarded. In contrast, in Eqn (6), the main term vanishes. Then, considering the next term of the expansion of the r.h.s. of Eqn (2) in small F, we get $a \approx -\mathrm{i}(F/G) + (F/G)^2$, and equality $\sigma_{\mathrm{ext}} = \sigma_{\mathrm{sca}}$ is restored.

As noted above, Eqns (3), (6) retain their form for an arbitrary function $\varepsilon(r)$. Note now that, in view of the scattering independence of each of the partial modes discussed above, for passive, i.e., noninverse populated particles,

the obvious inequality $\sigma^{(z)}_{n,\,\mathrm{ext}} \geqslant \sigma^{(z)}_{n,\,\mathrm{sca}}$ must hold. Hence, as follows from Eqns (3), (6), $\mathrm{Re}\, z_n \geqslant |z_n|^2$. Then, representing z as $z = z_0 \exp(\mathrm{i}\phi)$, we get $\cos\phi \geqslant z_0$, which leads to the conclusion $z_0 \leqslant 1$. This inequality gives rise to the following fundamental restriction for the partial extinction and scattering cross-sections for a given nth mode:

$$\sigma^{(n)}_{\mathrm{sca,\,max}} \leqslant \sigma^{(n)}_{\mathrm{ext,\,max}} \leqslant \frac{2(2n+1)\pi}{k^2}\,, \tag{7}$$

where the equalities of the three quantities can be achieved only at $z_0 = 1$ and $\phi = 0$, i.e., for a purely real scattering coefficient $z = 1$. On the other hand, at a purely real $z = 1$, we have $\sigma^{(z)}_{n,\,\mathrm{ext}} = \sigma^{(z)}_{n,\,\mathrm{sca}}$, that is, $\sigma^{(z)}_{n,\,\mathrm{abs}} = 0$, which corresponds to the nondissipative limit.

Thus, with the help of the above straightforward reasoning, we come to an essential fundamental conclusion: upon the scattering of a plane monochromatic linearly polarized wave by a particle with an arbitrary spherically symmetric dependence of its permittivity on r, at any value of the multipolarity, the partial extinction and scattering cross-sections satisfy inequalities (7). At the same time, the equalities can be achieved only in the nondissipative limit (cf. formula (10) obtained below). Of course, the converse is false — not any scattering in the absence of dissipation manifests the maximal values of the partial cross-sections.

Note also that, in the commonly used terminology, the Rayleigh approximation means not only ignoring F relative to G in the denominator of expression (2) for the scattering coefficients, but also disregarding the contributions to the scattering of all multipoles but the dipole. However, it will be convenient for us to use an extended interpretation of this term, which implies just ignoring F relative to G, while the higher-order multipoles may be counted. This makes it possible also to apply the term to any partial mode at $n > 1$.

Let us now discuss what happens when ε approaches $-(n+1)/n$ [28, 29]. As said above, we begin the discussion with the nondissipative limit of a purely real ε. Since we are interested in the close proximity of the point $\varepsilon = -(n+1)/n$, it is convenient to introduce $\delta\varepsilon \equiv \varepsilon + (n+1)/n$. Then, the leading order approximation in small $\delta\varepsilon$ for a_n reads

$$a_n \approx \frac{\mathrm{i}\gamma_n/2}{\delta\varepsilon + \mathrm{i}(\gamma_n/2)}\,, \quad \gamma_n = \frac{2(n+1)x^{2n+1}}{\left[n(2n-1)!!\right]^2}\,. \tag{8}$$

At any fixed x, for $|a_n|^2$ as a function of $\delta\varepsilon$, this expression leads to a Lorentzian profile with a linewidth equaling γ_n, while at $\delta\varepsilon \gg \gamma_n$ it gives rise to the formula

$$a_n \approx \frac{\mathrm{i}\gamma_n}{2\delta\varepsilon}\,; \tag{9}$$

at $n = 1$ (the dipole approximation), the above formula results in the same expression for the scattering cross-section as the one following from Eqn (1) at $|\varepsilon + 2| \ll 1$.

The finiteness of γ_n is strongly associated with the finiteness of x. Indeed, the discussed Rayleigh approximation corresponds to the polarization of a sphere in a spatially uniform electric field. Such a field may be regarded as that of an electromagnetic wave with an infinitely large wavelength. On the other hand, at the transition to the infinitely large wavelength, x, and with it γ_n, tends to zero. In other words, in the absence of dissipation, the finite linewidth occurs only beyond the framework of the Rayleigh approximation, when the departure of the incident wave field from the spatially homogeneous one (i.e., the retardation effect) is taken into account. This quantitative result entirely agrees with the qualitative reasoning about the radiative damping given above during the discussion of the Rayleigh formula.

It should also be emphasized that a 0/0 uncertainty appears for a_n given by Eqn (8) at $\delta\varepsilon = 0$ and $\gamma_n = 0$. This uncertainty cannot be resolved: at $\delta\varepsilon = 0$ and $\gamma_n = 0$, the r.h.s. of Eqn (8) has no limit, and the point itself is an analogue of essentially singular points of analytic functions. In the presence of finite dissipative damping, considered in the next Section 2.2.2, the singularity is smoothed out. Instead, a region with a sharp variation of the scattering coefficients comes into being. However, as long as the dissipation is weak, the size of this region is small. Then, the study of the nondissipative limit, as usual, helps to draw a correct conclusion about the behavior of the scattering coefficients in this case too; see more below, as well as the Appendix and Ref. [30].

We emphasize that the occurrence of such a feature is not a unique peculiarity of the scattering problem under consideration. It has a very general nature and occurs in a broad class of resonant phenomena when the corresponding dissipative constants tend to zero.

It is important to note that, since F_n and G_n are the functions of two independent variables x and mx, i.e., in fact, x and ε, at a purely real ε, the resonance condition $G^{(a)}_n = 0$ sets on the plane x, ε a certain resonance curve $\varepsilon = \varepsilon^{\mathrm{res}}(x)$. At each point on this curve, the scattering coefficient reaches its maximum, $a_n = 1$. The point $x = 0$, $\varepsilon = -(n+1)/n$, discussed above is just the starting point of this curve, from which it begins at $x = 0$.

At small but finite x, the quantity $\delta\varepsilon$ in expression (8) should be understood as $\varepsilon - \varepsilon^{\mathrm{res}}(x)$. Similarly, in expression (4), we should set $\varepsilon = \varepsilon^{\mathrm{res}}(x)$. However, calculations show that the difference between $\varepsilon^{\mathrm{res}}(x)$ and its value at $x = 0$ turns out to be of the order of x^2 [29]; see also Eqn (5). Then, the replacement for $\varepsilon^{\mathrm{res}}(x)$ by its value at $x = 0$, i.e., by $-(n+1)/n$, results in just small corrections to expression (8) for γ_n. Thus, at a small but finite x, in the leading approximation, neither the position of the resonance point on the ε axis nor the width of the resonance lineshape (x) changes with respect to their values at $x = 0$. This is grounds to disregard the higher-order terms in expressions (4), (5).

To apply this result to an actual physical problem, one should change the independent variables from x, ε to R, ω and consider the shape of the line as a function of ω at a fixed R. This is easy to do by expanding $\varepsilon(\omega)$ in series about the point $\omega = \omega_n^{\mathrm{res}}$, where $\varepsilon(\omega_n^{\mathrm{res}}) = \varepsilon^{\mathrm{res}}(x)$ is defined by the condition $\varepsilon(\omega_n^{\mathrm{res}}) = \varepsilon^{\mathrm{res}}(x)$. In this case, $\delta\varepsilon \to (\mathrm{d}\varepsilon/\mathrm{d}\omega)_{\omega_n^{\mathrm{res}}}\delta\omega$, where $\delta\omega = \omega - \omega_n^{\mathrm{res}}$. As for x, in the leading approximation, it can be represented as $k(\omega_n^{\mathrm{res}})R \equiv m_{\mathrm{out}}\omega_n^{\mathrm{res}}R/c$. As a result, we again obtain a Lorentzian profile, but this time it is for the function $|a_n(\delta\omega)|^2$.

According to formula (3), the same Lorentzian profile is preserved for the partial cross-section. In full accordance with the general principles set forth above, the resonance point is defined as the point at which this profile has a maximum, $a_n = 1$, and the partial cross-section is

$$\sigma^{(a)}_{n,\,\mathrm{sca,\,max}} = \frac{2(2n+1)\pi}{k^2}\,, \tag{10}$$

cf. Eqn (7).

Another important feature of this resonance scattering is an unusual dependence on x of the components of the electric and magnetic fields of the partial scattered wave in the immediate vicinity of the particle's surface. In the Rayleigh

case, they are estimated by the expressions $E_{r,\theta,\varphi}^{\mathrm{sca}\,(n)} \sim x^{n-1}$, $H_{\theta,\varphi}^{\mathrm{sca}\,(n)} \sim x^{n}$, $H_{r}^{\mathrm{sca}\,(n)} \sim x^{n+1}$, i.e., they remain regular at $x \to 0$. At the resonant scattering when moving in the plane ε, x along the resonant curve in the direction $x = 0$, these quantities are estimated as $E_{r,\theta,\varphi}^{\mathrm{sca}\,(n)} \sim x^{-(n+2)}$, $H_{\theta,\varphi}^{\mathrm{sca}\,(n)} \sim x^{-(n+1)}$, $H_{r}^{\mathrm{sca}\,(n)} \sim x^{n+1}$, i.e., with the exception of the radial component of the magnetic field, they are singular in x and increase as the size of the scattering particle decreases [29, 31]. This property is a direct consequence of the independence of $\sigma_{n,\mathrm{sca,max}}^{(a)}$ from x; in order to provide constant power of scattered radiation with a reduction in the size of the radiating area, it is required to increase the amplitude of the fields in this area.

In the above reasoning, we imply that, at the size parameter tending to zero, the problem continues to be described within the framework of the macroscopic approximation and classical electrodynamics adopted here. Since $x = kR$, its vanishing can occur either by increasing the radiation wavelength and then reaching the long-wavelength microwave range or reducing the particle size. While the former does not drive us beyond the accepted problem formulation, this is not the case for the latter. When the particle size is reduced to a (sub)nanometer range, the problem description should take into account some new effects, including quantum ones. This may radically alter the particle interaction with the electromagnetic radiation discussed here. However, covering these fascinating and important issues lies beyond the scope of this review. †

It would then seem that the mentioned independence $\sigma_{n,\mathrm{sca,max}}^{(a)}$ from x leads to a paradox: a particle of zero size, i.e., actually nonexisting, still has a finite scattering cross-section, which, obviously is nonsense. On the other hand, this ridiculous conclusion is based on an analysis of the exact solution to the problem, and, therefore, to the same extent may be applied to Maxwell's equations themselves, the validity of which no one, of course, doubts. The mentioned fact that a very small value of R drives the problem beyond the framework of its applicability does not save the day either, because, as indicated, the transition $x \to 0$ can occur due to an increase in the radiation wavelength, which does not violate the applicability conditions. Therefore, we must find the paradox resolution within the given problem formulation. We will return to this issue a little later; in the meantime, let us continue our analysis.

As was qualitatively shown in the discussion of Eqn (1) and quantitatively proved based on the exact Mie solution, at $x \ll 1$, the dipole mode makes the main contribution to the Rayleigh scattering. Partial cross-sections of higher multipoles decrease as $x^{2(2n+1)}$; see Eqns (2)–(5). On the contrary, upon resonant scattering, the partial cross-sections increase with an increase in n as $2(2n+1)$; see Eqn (10). In other words, the resonant value of the partial cross-section of the dipole mode is less than that for the quadrupole, which, in turn, is less than that for the octupole, etc. Thus, during resonance scattering, an inverted hierarchy of resonances [28, 32] occurs. It should be emphasized that, since for every value of n the resonant values of ε are different ($\varepsilon^{\mathrm{res}} \approx -(n+1)/n$), and the resonant lines are narrow, overlapping resonances of different orders does not occur, and the inverted hierarchy does not affect the convergence of the multipole expansion for the sphere.

† Thus, in what follows, it is supposed that the transition $x \to 0$ occurs owing to the first option. (*Authors' note to English proof.*)

It should also be kept in mind since every multipole has its own resonant value of ε, it has its own resonant frequency. Therefore, when we talk about the inverted hierarchy of resonances, we mean a comparison of the cross-sections at different values of ω — their own ones for every resonance. In this case, the proportionality of the partial cross-sections to $2(2n+1)$ is preserved only if k remains unchanged; see Eqn (10). Since the comparison takes place at different frequencies, the invariability of k can be maintained only by comparing the resonant cross-sections for spheres with different sizes. Such a comparison, to put it mildly, looks somewhat strange. It is, therefore, desirable to understand how the scattering cross-section for the same particle changes when its size is fixed, and the only variable parameter is the frequency of incident radiation.

As is well known for Rayleigh scattering, if one ignores the dispersion of permittivity, then, at a fixed R, the scattering cross-section is a continuous function of the frequency and increases with an increase in the latter as ω^4 for the dipole mode, and as ω^{4n} for higher multipoles; see (3), (4). Regarding resonant scattering, due to the narrowness of resonance lines, this scattering is concentrated in the small vicinity of the resonant frequencies; therefore, the dependence of its cross-section on ω is discrete and is determined by the spectrum of resonant frequencies.

In general, the frequency dependence is as follows. There is a relatively wide dipole resonance line, the wings of which correspond to the Rayleigh dependence; see Eqn (1). On these wings, as on a pedestal, narrow intense spikes corresponding to the resonant scattering rise. Their width decreases as n increases. The details of such a pattern are determined by a specific type of permittivity dispersion, $\varepsilon(\omega)$.

As an example, we present the total scattering cross-section $\sigma_{\mathrm{sca}}(\omega) = \sum_n \sigma_{n,\mathrm{sca}}(\omega)$ calculated at a fixed R on the basis of the exact Mie solution, for the permittivity dispersion law described by Drude's formula. For the nondissipative case considered here, it has the form

$$\varepsilon = 1 - \frac{\omega_{\mathrm{p}}^2}{\omega^2}, \quad \omega_{\mathrm{p}} = \mathrm{const}\,. \tag{11}$$

However, since in the next Section 2.2.2 we will discuss the effects of finite dissipation, it makes sense to give this formula in a more general form, namely,

$$\varepsilon = 1 - \frac{\omega_{\mathrm{p}}^2}{\omega(\omega + \mathrm{i}\nu)}, \quad \omega_{\mathrm{p}} = \mathrm{const}, \ \nu = \mathrm{const}\,. \tag{12}$$

Here, ω_{p} and ν denote the plasma and collision frequencies, respectively.

For $\varepsilon(\omega)$ described by Eqn (11), the condition $\varepsilon = -2$ (dipole resonance at $r \to 0$) is fulfilled at $\omega = \omega_{01} = \omega_{\mathrm{p}}/\sqrt{3}$. It is convenient to carry out the further consideration in terms of the dimensionless scattering efficiency $Q_{\mathrm{sca}} = \sigma_{\mathrm{sca}}/(\pi R^2)$. As for the size parameter x, it can be written as $x = x_{01}\omega/\omega_{01}$ so that $x = x_{01}$ at $\omega = \omega_{01}$.

Note that, although our analysis is based on the expansion of the scattering coefficients in a small size parameter and is formally applicable only at $x \ll 1$, in fact, the obtained results remain valid up to $x \sim 1$. To illustrate this statement, we calculate the efficiency of the extinction cross-section at $x_{01} = 0.9$; see Fig. 1 (we recall that, in the absence of dissipation, the extinction and scattering cross-sections are identical).

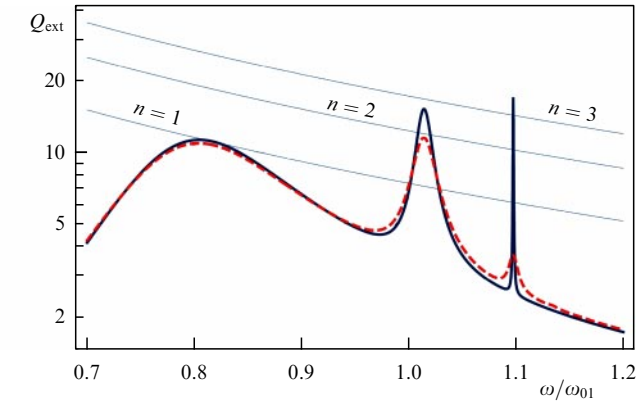

Figure 1. Dispersion law for particle's extinction efficiency $Q_{ext}(\omega)$, on logarithmic scale (solid line). Nondissipative limit, corresponding to Drude's formula (11). Calculation based on the exact Mie solution at $x_{01} = 0.9$. Thin inclined lines display the maximal values for the partial efficiencies of dipole ($n = 1$), quadrupole ($n = 2$), and octupole ($n = 3$) resonances calculated by formula (10) and equal to $2(2n+1)\omega_{01}^2/(x_{01}\omega)^2$. At the resonances, maxima of the total extinction efficiency $Q_{ext}(\omega)$ are greater than corresponding maxima of partial efficiencies due to finite contribution of nonresonant modes. Dotted line shows the same dependence $Q_{ext}(\omega)$ when finite dissipation is taken into account, and $\varepsilon(\omega)$ is determined by Eqn (12) at $\nu = 0.01\omega_{01}$. See main text for details.

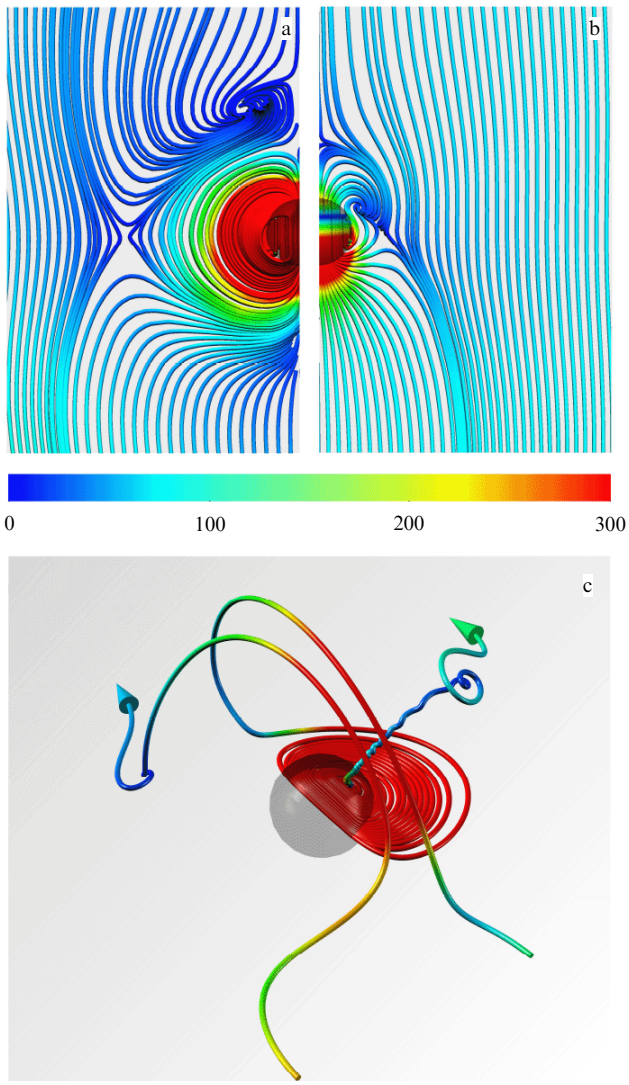

Figure 2. (Color online.) 'Streamlines' of the Poynting vector in the vicinity of dipole resonance. Value of the Poynting vector at every point of the streamlines is shown in color. Color scale is normalized to the intensity of the incident wave and is common to all panels. Scattering spherical particle is shown translucent to trace the path of lines inside it; $x = 0.3$; $\mathrm{Re}\,\varepsilon = -2.17$. With this x, the resonance point corresponds to $\mathrm{Re}\,\varepsilon = -2.22$. (a) Nondissipative limit: $\mathrm{Im}\,\varepsilon = 0$ left half-plane. Incident plane wave propagates from the bottom edge of the panel to the top. Vector **E** lies in the plane of the figure. Lines shown lie in a thin layer that includes the sphere's equatorial section. Layer lies in the plane of the drawing. Line break indicates that the streamlines go out of the horizontal boundaries of the layer. The 'funnel', as well as the optical vortex (singular focus-saddle point) and energy circulation around the center of the localized plasmon, are clearly visible. (b) Right half-plane for the same case as shown in Fig. 2a but with dissipation taken into account: $\mathrm{Im}\,\varepsilon = 0.18$. With this set of parameters, the case approximately corresponds to an aluminum nanoparticle with $R = 6.8$ nm. (c) Nondissipative limit with the same set of parameters as that in the case shown in Fig. 2a. Two characteristic substantially three-dimensional streamlines whose origins are situated slightly above the equatorial plane of the particle.

Although the size parameter is not small anymore, the plot $Q_{ext}(\omega)$ is entirely consistent with the above description. The shown frequency interval covers the first three resonances, namely the dipole ($n = 1$) at $\omega/\omega_{01} \approx 0.804$, quadrupole ($n = 2$) at $\omega/\omega_{01} \approx 1.014$, and octupole ($n = 3$) at $\omega/\omega_{01} \approx 1.097$. The resonance lines of the quadrupole and octupole modes are located on the wing of the dipole resonance line. Both the inverted hierarchy of resonances and sharp narrowing of the resonance lines with an increase in n are clearly visible (note the logarithmic scale of the plot); cf. expressions (8), (10).

The fact that the size parameter is of the order of unity manifests itself only in a significant redshift of the resonant frequencies relative to their values at $R = 0$, so that the quadrupole resonant frequency at $x_{01} = 0.9$ almost coincides with the dipole resonant frequency (ω_{01}) at $x_{01} = 0$. Another peculiarity of $Q_{ext}(\omega)$ at $x \sim 1$ is that, due to the contribution of the wings of the nonresonant modes, which at such a value of x decay quite slowly, the total extinction efficiency at the resonance point is noticeably greater than the maximal value for the partial efficiency of the corresponding resonant mode determined by Eqn (10).

For comparison, Fig. 1 represents the same dependence $Q_{ext}(\omega)$ when finite dissipation is taken into account, and $\varepsilon(\omega)$ is determined by Eqn (12) at $\nu = 0.01\omega_{01}$. Such a collision rate at room temperature is typical for metals with low dissipation in the vicinity of the Mie resonance frequencies (potassium, sodium, aluminum). As usual, the higher the Q-factor of the resonance in the nondissipative limit, i.e., the narrower its line, the more pronounced the dissipation effects. A more detailed discussion of $Q_{ext}(\omega)$ in the presence of dissipation will be given in the next Section 2.2.2.

However, perhaps the most exciting characteristic of resonant scattering is the topological structure of the Poynting vector field describing the circulation of energy in the vicinity of the scattering particle. Since the size of the particle is small relative to the radiation wavelength, the radius of the sphere R becomes the only characteristic scale that determines the structure of the field in the vicinity of the particle. Nonetheless, within this scale, the field has a complex structure containing various singular points (this is very unusual for a particle of subwavelength dimensions). The number, type, and spatial position of these singularities are highly susceptible to very slight variations in the frequency of the incident radiation and associated changes in ε [29, 33–36].

Table. Comparative characteristics of Rayleigh and anomalous scattering.

Characteristics	Rayleigh scattering	Anomalous scattering
Hierarchy of resonances	Normal (amplitudes decrease with increase in n)	Inverted (amplitudes increase with increase in n)
Dependence on R	$\sigma_{n,\mathrm{sca}}^{(a)} \sim R^{2(2n+1)}$	$\sigma_{n,\mathrm{sca}}^{(a)}$ does not depend on R
Frequency dependence	Continuous	Discrete
Amplitudes of scattered field near the sphere	**E** and **H** smooth in R at $R \to 0$	**E** and **H** singular in R at $R \to 0$
Poynting vector field	Simple structure. May exhibit saddle-type singularities [33]	Complex structure. May exhibit various singularities, including optical vortices

As an example, Fig. 2 shows streamlines of the Poynting vector field in the vicinity of dipole resonance obtained by the authors of the review as a result of direct numerical integration of Maxwell's equations with the help of the *CST Studio Suite package*. All the parameters are specified in the figure caption. At every point of the streamlines, the Poynting vector is directed tangentially to them. Figure 2a, b shows the field structure in the **E**-plane of a linearly polarized incident electromagnetic wave. Of course, the field structure is symmetric with respect to the perpendicular plane passing through the center of the particle (in the given case, it is the **H**-plane of the incident electromagnetic wave). For this reason, Fig. 2a shows only the left half of the overall picture, which corresponds to the nondissipative limit. For comparison, Fig. 2b shows the right half of a similar picture when the dissipation is taken into account.

It is seen that the field structure forms a 'funnel', which 'draws' the field from a large area of space located 'downstream' and transports it to a small spatial area in the proximity of localized plasmons. The funnel effect also provides a large concentration of the electromagnetic energy in the particle, necessary to maintain high intensity of the scattered radiation; see the scale of the color bar in the figure.

Note also a center-type singular point (see Fig. 2a) lying on the surface of the particle and corresponding to the center of the localized plasmon. In the vicinity of this point, the streamlines are closed curves. This means that the electromagnetic field is entirely confined in the area of space filled with such lines — energy can neither enter this area nor be emitted from it. How does it get in? After all, before the particle begins to be irradiated by an incident wave, there is no field in this area. Obviously, the accumulation of the electromagnetic energy there could only happen at an initial stage of the irradiation process, when the scattering was essentially nonstationary, the resonance modes were still 'swinging' by the incident wave, and the field structure was significantly different from that shown in Fig. 2a. Here, we enter a new and fascinating area of nonstationary resonance effects in light scattering by nano-objects [37–39]. Unfortunately, due to the mentioned limitations we have placed on the scope of this review, we cannot afford to discuss these effects in any detail.

Let us get back to the analysis of the field structure shown in Fig. 2. The shape of the streamlines in the three-dimensional space when these lines do not belong to the invariant equatorial plane passing through the sphere's center is even more complex than the flat picture shown in Fig. 2a, b. For example, Fig. 2c shows two characteristic substantially three-dimensional streamlines of such a kind, originating slightly above the equatorial plane of the particle. The streamlines 'winding up' on the centers of the localized plasmons eventually abruptly leave this area in the transversal direction, creating some kinds of vortex protuberances (nano-projectors!). We emphasize that, at the given value of x, the wavelength of the incident radiation is more than twenty times larger than the sphere's radius, so that the entire complex field structure shown in the figure has a significantly subwavelength scale.

The presence of small dissipation does not lead to qualitative changes in this picture, except that, due to the energy conservation law, the emergence of streamlines closed on themselves becomes impossible, and singular center-type points turn into focuses (cf. Fig. 2a and b). However, as dissipation grows, the singular points sequentially disappear, and, ultimately, a fairly simple field structure characteristic of Rayleigh scattering comes into being [33].

Such a large number of qualitative differences between this resonant scattering and the Rayleigh one was the basis for assigning it the term *anomalous scattering* [32]. For the convenience of the reader, these differences are summarized in the table. It is assumed in the table that the frequency of the incident wave lies precisely in the center of the corresponding resonant line.

2.2.2 Finite dissipation effects. What happens in the case of finite but small dissipation? In the presence of dissipative losses, the dielectric constant becomes a complex quantity: $\varepsilon = \varepsilon' + \mathrm{i}\varepsilon''$. If dissipation is small ($0 < \varepsilon'' \ll 1$), then its treatment is reduced to a trivial replacement in expression (8) of the real $\delta\varepsilon$ by a complex one: $\delta\varepsilon' + \mathrm{i}\varepsilon''$. This leads to an increase in the width of the line, which is manifested in the replacement in the denominator of γ_n by $\gamma_n + 2\varepsilon''$, where the first term describes the nondissipative radiative damping, and the second one is related to conventional dissipative losses.

Obviously, the anomalous scattering can be realized, provided the radiative damping prevails over the dissipative one, i.e., at $\gamma_n \gg \varepsilon''$. In the opposite limiting case, the radiative damping can be disregarded. It is easy to see that ignoring the radiative damping is equivalent to ignoring F relative to G in Eqn (2), that is to say, to the Rayleigh approximation. The transition from one case to the other occurs at [28]

$$\varepsilon'' \sim \frac{(n+1)x^{2n+1}}{\left[n(2n-1)!!\right]^2}\,. \tag{13}$$

From Eqn (13), it becomes clear that there is no need to generalize our reasoning to the case of considerable values of ε'', when moving to substantial dissipation, the Rayleigh scattering is restored, and the question about the generalization is removed of its own accord.

Expression (13) also resolves the paradox about the finite scattering cross-section for a particle of zero size, noted in the

previous subsection. The paradox exists solely in the nondissipative limit. On the other hand, this limit is an idealization that is never realized in nature. There is no complete absence of dissipative processes. Accordingly, in any actual case, the imaginary part of permittivity may be very small, but it is always finite. Then, at any small but fixed value of ε'', as x decreases, a transition from anomalous to Rayleigh scattering occurs, i.e., at $x \to 0$, the scattering cross-section tends to zero, in full accordance with formula (1) and common sense.

Another independent mechanism of the paradox being resolved is associated with the sharp narrowing of the resonant linewidth at $x \to 0$; see Eqn (8). Since any actually existing radiation source has a finite linewidth, at a sufficiently small value of x, the value of γ_n inevitably becomes smaller than the source's linewidth, so that only a part of the radiation is scattered resonantly. At $x \to 0$, this part tends to zero, which also results in the vanishing of the corresponding cross-section [30].

This is well illustrated by the profiles shown in Fig. 1. At the given values of the problem parameters, the radiative damping in the dipole resonance region prevails over the dissipative one, and the shape of the line in the dissipative case barely differs from the nondissipative limit. In the region of quadrupole resonance, the dissipation effect is more pronounced, which leads to a decrease in the Q-factor of the resonance compared to the nondissipative limit. Finally, in the region of octupole resonance, the dissipative damping plays an overwhelming role, which leads to a radical drop in the Q-factor.

So far, we have discussed a spatially homogeneous particle. Recently, much attention has been paid to two-layer core–shell particles and their multilayer generalizations — shell particles consisting of several layers with different optical properties [40–45]. With a concentric arrangement of the layers, the problem of scattering of a plane monochromatic linearly polarized electromagnetic wave by such a particle also allows an exact solution by the same multipole expansion method. A sufficiently detailed discussion of this solution can be found, for example, in Ref. [41].

It is essential that, in this case, the scattered field outside the particle be presented by the same multipole expansion as that for a homogeneous sphere. Therefore, as already noted above, expressions (3), (6), linking different partial cross-sections with the scattering coefficients remain unchanged. Regarding the scattering coefficients themselves, they still retain the same fundamental structure defined by Eqn (2). However, the complexity of a specific expressions for the functions F_n, G_n increases with an increase in the number of layers (in the general case of an arbitrary number of layers, the scattering coefficients are determined through certain recurrence relations).

An essential difference between light scattering by such a particle and the above case of a homogeneous sphere is that now the problem acquires a qualitatively new property. Variations in the radii of the core and shell layers and/or their permittivity makes it possible to shift the positions of different resonances and ensure that several different resonances can be excited at the same frequency (overlapping resonances).

Owing to the linearity of the problem and the orthogonality of the eigenmodes, the partial cross-sections of various resonances add up. Each resonance can be optimized to maximize the corresponding partial scattering cross-section. By combining the optimization conditions with the overlapping requirements for different resonances, it is possible to design a super-scattering core-shell structure whose total scattering cross-section significantly exceeds the maximum value for a single partial mode; see Ref. [46] for more detail.

Concluding the discussion of the theoretical description of anomalous scattering, we will consider what differences arise when an infinite circular cylinder scatters light. Almost everything said about a spherical particle is transferred to the scattering of light by the cylinder without significant changes [47–49]. However, there is one qualitative difference between these two cases: if for a sphere at $x \to 0$ the resonant values of ε for various multipoles differ from each other, and there is no overlap of resonances, then, for a cylinder in the same limit, resonant ε for all n except $n = 0$ is the same and equal to -1. In such a case, a question arises as to the convergence of the multipole expansion at $\varepsilon \to -1$, $x \to 0$. This issue is studied in detail in Ref. [30]. It is shown that, for the scattering coefficients, the point $\varepsilon \to -1$, $x \to 0$ is an analog of essential singular points of analytic functions, so that the scattering coefficients do not have a definite limit at this point (see also the Appendix). To overcome the resulting problem, as noted above, one should go beyond the monochromatic approximation and take into account the finiteness of the width of the source line, after which several limits have to be found in the correct sequence. The result is a well-defined expression for the scattering cross-section, which turns to zero when $x \to 0$.

Let us also point out that the problem of anomalous scattering by a cylinder has a long history that is unexpected for the optical community. It is connected with the radio sondage of meteor tracks in the atmosphere [50–52]. Moving at cosmic speeds through Earth's atmosphere, meteors create an almost ideal cylindrical track of ionized air, which in some cases can be considered to be collisionless plasma. The resonant frequencies of such a cylinder lie in the microwave range. Irradiated by radar with a radio wave at the corresponding resonant frequency, the track produces a powerful reflected signal that fully corresponds to the anomalous scattering discussed above. One can get thorough information about the original meteor by studying this signal. A detailed discussion of these issues lies outside the scope of this review.

3. Maximization of light absorption by a subwavelength particle. Anomalous absorption

Another significant range of issues is related to the energy release occurring in an irradiated subwavelength particle due to the absorption of incident light. In particular, we will be interested in the problem of maximization of energy release [53], essential for many applications: in diagnosing and treating certain diseases (especially oncological), microsurgery, the problem of high-density recording of information (the heating of nanoparticles above the Curie temperature leads to local demagnetization of magnetic materials), etc. [54–59].

Of course, when it comes to applications, it is much more important to know to what temperature a particle is heated, rather than what amount of energy it absorbs. The temperature is described by a solution (in both the particle itself and its ambient medium) to the complete set of Maxwell's

equations supplemented by those of the heat transfer. However, Maxwell's equations are decoupled from the heat transfer ones in a linear problem. The solution to the electromagnetic part of the problem is included in the one of heat transfer only in the form of a source and does not depend on the latter's solution. Since the problem of heat transfer lies outside the scope of this review, we will limit ourselves only to an inspection of the energy release. As for the full version of the problem, including the heat transfer, its discussion can be found, for example, in Refs [60–62].

At first glance, the problem of absorption maximization is trivial. For the considered nonmagnetic materials, the density of energy release due to dissipative losses is proportional to $\varepsilon''|\mathbf{E}|^2$: the greater the imaginary part of the permittivity, the greater the absorption [23].

In fact, the issue is somewhat more complicated: $\mathbf{E}$, which is included in this expression, is a field at the point in space where the energy density is calculated. The energy release occurs inside the particle; hence, $\mathbf{E}$ is the field *inside* the particle.

At a resonance, the field inside the particle increases. Let us consider the excitation of resonant modes by an external field as forced vibrations of a harmonic oscillator. Then, in a stationary state, the amplitude of the vibrations at the resonance point is in inverse proportion to the dissipative constant. In our case, this means that, in the vicinity of the resonance, the field inside the particle is estimated in the order of magnitude by the expression $\mathbf{E}_0/\varepsilon''$, where $\mathbf{E}_0$ stands for the amplitude of the incident wave field. As a result, the density of the energy release is proportional to $|\mathbf{E}_0|^2/\varepsilon''$.

Thus, we arrive at the opposite conclusion: to maximize the energy release, we must make the sphere of a material with as small dissipation as possible and, at the same time, keep the radiation frequency in the vicinity of the resonant one.

Recall now the results of the previous section: with a decrease in ε'', scattering in the vicinity of resonances inevitably becomes anomalous; see Eqn (13). Therefore, to treat the absorption maximization problem accurately, it is again necessary to consider the exact solution to the scattering problem.

It is easy to do. According to the exact solution, the absorption partial cross-section for a sphere is described by the following expression [1, 3]:

$$\sigma_{n,\,\mathrm{abs}} = \frac{2(2n+1)\pi}{k^2}\left[\left(\operatorname{Re} a_n - |a_n|^2\right) + \left(\operatorname{Re} b_n - |b_n|^2\right)\right]. \qquad (14)$$

Bearing in mind wider applications of the results, we will not limit ourselves to the assumption of smallness of x. Since electric and magnetic modes are independent, the problem of the $\sigma_{n,\,\mathrm{abs}}$ maximization is reduced to finding the maximum of the expression $z_n' - z_n'^2 - z_n''^2$, where, instead of z_n, any of the coefficients a_n and b_n may stand. It is easy to see that the maximum of this expression is $1/4$, being achieved at $z_n'' = 0$, $z_n' = 1/2$. In this case, the value of the absorption partial cross-section is equal to the scattering partial cross-section, equal to $\sigma^{(z)}_{n,\,\mathrm{sca},\,\max}/4 \sim 1/k^2$ and does not depend on radius R; see Eqn (10).

This result is equivalent to the well-known antenna theory criterion for maximizing the power transmitted from a radiation source to its receiver [63, 64]. From it, in particular, it follows that the effective area of a small resonant antenna (absorption cross-section) turns out to be of the order of the square of the wavelength of the radiation and does not depend on the size of the antenna — otherwise, a handheld transistor receiver could not receive radio transmissions in the meter range! Compare it with the outcome discussed above for the anomalous absorption: $\sigma_{\mathrm{abs}} \sim 1/k^2$.

It is also helpful to emphasize that, although, in the general case, the scattering coefficients are complex, at the maximum of scattering (at zero dissipation) and the maximum of absorption (at finite dissipation), they become purely real quantities equal to 1 and $1/2$, respectively.

Note that, with complex ε, the functions F and G in expression (2) become complex. Presenting them as $F = F' + \mathrm{i}F''$, $G = G' + \mathrm{i}G''$, we may rewrite expressions (2) for the scattering amplitudes as follows:

$$z_n = \frac{F_n' + \mathrm{i}F_n''}{F_n' - G_n'' + \mathrm{i}(F_n'' + G_n')}. \qquad (15)$$

In this case, after simple calculations, the absorption maximum conditions ($z_n' = 1/2$, $z_n'' = 0$) are rewritten as reciprocity relations: $F_n' = -G_n''$, $F_n'' = G_n'$.

Significantly, for the same reasons as those discussed above in connection with anomalous scattering, expressions (14), (15) and all of the conclusions following from them remain valid with an arbitrary spherically symmetric dependence on the coordinate r of permittivity of the scattering sphere, including a stepwise dependence — layered structures. More general results on the scattering and absorption of light by a particle of an arbitrary shape are contained in Refs [65–67].

Now let us employ the smallness of the size parameter x. As already noted, in this case, at any n, the functions G_n for the magnetic modes are of the order of unity and do not vanish anywhere, while the functions F_n are small. As a result, the absorption associated with the excitation of the magnetic modes is negligible and, therefore, of little interest to us.

Regarding the electric modes, according to Eqns (4), (5), at $\varepsilon'' \ll 1$ in the leading approximation, F_n can be considered a purely real quantity, i.e., in the reciprocity relations, one can put $F_n'' = 0$. From this, it immediately follows that $G_n' = 0$, which exactly coincides with the condition of maximizing the anomalous scattering in the absence of dissipation. The second reciprocity relation $F_n' = -G_n''$, taking into account Eqns (4), (5), leads to the conclusion that the absorption maximum is realized precisely in the middle of the transition region from anomalous to Rayleigh scattering, when in formula (13) the $\sim$ sign is replaced by an equal sign, and the contributions made to the linewidth by the radiation and dissipative damping are equal to each other.

Thus, for a subwavelength particle, the maximum of the partial absorption cross-section is associated with the resonance excitation of the electric modes and is achieved at a small value of the imaginary part of the dielectric constant. In this case, the scattering itself is close to anomalous and essentially inherits all its features; see the Table. Such absorption is also naturally called anomalous [31].

What about the shape of the lines at the anomalous absorption? First of all, note that, at a sharp resonance, the linewidth is determined by the behavior of the denominator of expression (2). The denominators of the partial scattering and absorption cross-sections are the same; see Eqns (3), (14). Therefore, both lines have the same shape and are distinguished only by a scale factor. If, as is customary, the shape of the line means the dependence of the corresponding partial cross-section on ω, then there is nothing new for the case in question. In fact, this issue was already discussed

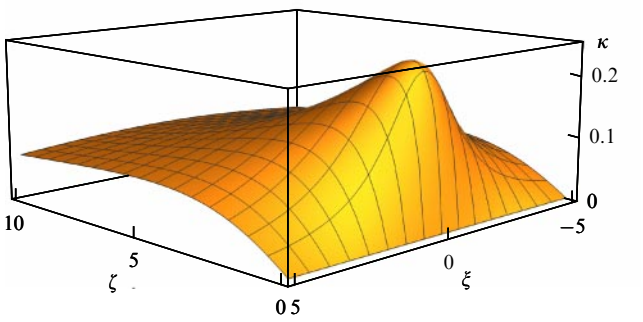

Figure 3. Universal surface $\kappa = \kappa(\xi, \zeta)$; see main text for details.

in Section 2.2, where it was shown that the line has a bell-shaped Lorentzian profile, and its width (including the contribution of the dissipative damping) was already determined. These results are transferred to the present case without any changes.

However, it is reasonable to extend the standard line-shape definition and consider $\sigma^{(a)}_{n,\mathrm{abs}}$ to be a function of two independent variables, ε' and ε'', i.e., a function of a complex ε. Taking advantage of the fact that, for a subwavelength particle in the leading approximation F_n are purely real functions and $G_n \sim \delta\varepsilon \equiv \delta\varepsilon' + \mathrm{i}\varepsilon''$, in the vicinity of the absorption maximum, it is convenient to introduce, instead of $\sigma^{(a)}_{n,\mathrm{abs}}$, ε', and ε'', new dimensionless quantities:

$$\kappa = \frac{x^2 \sigma^{(a)}_{n,\mathrm{abs}}}{2(2n+1)\pi R^2}, \quad \xi = -\frac{G_n^{(a)\prime}}{F_n^{(a)\prime}}, \quad \zeta = -\frac{G_n^{(a)\prime\prime}}{F_n^{(a)\prime}}. \tag{16}$$

To avoid misunderstandings, note that, due to the reciprocity relations and the fact that $G_n'' \sim \varepsilon'' > 0$, at the absorption maximum, $F_n^{(a)\prime} = -G_n^{(a)\prime\prime} < 0$. By continuity, F and G retain the same signs in the vicinity of the maximum too, so that $\zeta > 0$.

It is easy to see that, in this case, at any n, the surfaces $\sigma^{(a)}_{n,\mathrm{abs}}(\varepsilon', \varepsilon'')$ are reduced to a single universal surface described by the equation [31]

$$\kappa = \frac{\zeta}{(1+\zeta)^2 + \xi^2}, \quad \zeta > 0. \tag{17}$$

This surface is shown in Fig. 3. Note that, if sections of the surface $\kappa = \kappa(\xi, \zeta)$ with the planes $\zeta = \mathrm{const}$ gives a symmetrical Lorentzian profile, the ones with the planes $\xi = \mathrm{const}$ generate a family of strongly asymmetric curves. Every one of them exhibits a sharp decay when ζ changes from the point corresponding to the maximum of the profile in the direction of decrease in ζ and a long, slowly decaying tail when changing ζ in the opposite direction; see also [68].

4. Anomalous absorption and actual materials

The reasoning given in the previous sections tacitly assumed that the most important thing was to determine the appropriate conditions for implementing the effects discussed there. After this is done, the rest is trivial — one just needs to select a suitable sample to observe these effects. However, the trouble is that, if we leave aside artificial metamaterials specially made to have given properties and limit ourselves to ordinary ones existing in nature, they have a specific fixed dispersion law $\varepsilon(\omega)$. Therefore, the challenge is not to select a suitable

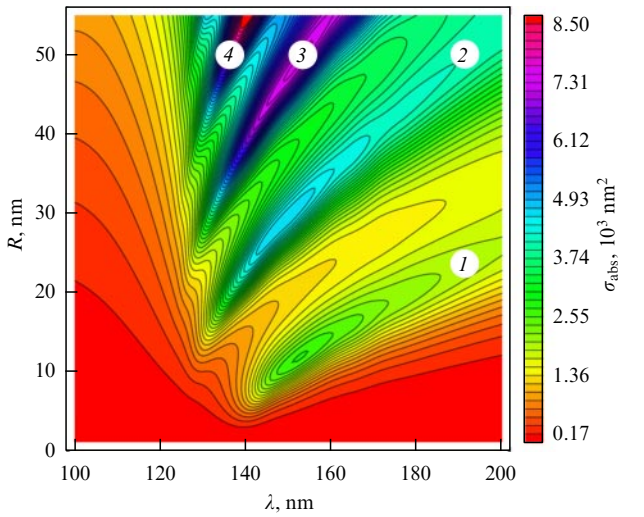

Figure 4. Absorption cross-section of an aluminum sphere as a function of its radius and wavelength. Calculations are made according to the exact Mie solution with actual optical properties of aluminum nanoparticles [31]; see main text for details. Regions with preferential contributions of dipole ($n = 1$), quadrupole ($n = 2$), octupole ($n = 3$), and hexadecapole ($n = 4$) modes are marked with numbers *1*, *2*, *3*, and *4*, respectively. Inverted hierarchy of resonances is clearly visible.

sample, but to understand if there is any material with the required dependence $\varepsilon(\omega)$. This problem has been discussed in detail in our publications [31, 65], but now the discussion manner adopted there seems to us clumsy, and, below, we will apply another, equivalent, approach.

As shown above, the anomalous absorption conditions assume that, in this case, $\mathrm{Re}\, a_n = 1/2$, $\mathrm{Im}\, a_n = 0$. On the other hand, the scattering coefficients are certain functions of the problem's parameters, uniquely defined by the exact Mie solution, according to which $a_n = a_n(x, mx)$; see the Appendix. For the sake of simplicity, consider a particle irradiated in a vacuum, so that $m_{\mathrm{out}} \equiv 1$. In this case, $m = \sqrt{\varepsilon}$ is uniquely determined by the dispersion dependence of the particle's material. In the case of a nanoparticle, it may be supplemented by a dependence on the particle size R. As a result, the conditions for the anomalous absorption acquire the form

$$\begin{aligned} \mathrm{Re}\left[a_n\left(\frac{R\omega}{c}, \varepsilon(\omega, R)\right)\right] &= \frac{1}{2}, \\ \mathrm{Im}\left[a_n\left(\frac{R\omega}{c}, \varepsilon(\omega, R)\right)\right] &= 0. \end{aligned} \tag{18}$$

These conditions, considered as equations, must define discrete pairs ω and R for which anomalous absorption is realized. Alas, it has not yet been possible to find a single actual material for which these equations would have a solution in the optical frequency range. Does this mean that the anomalous absorption remains a hypothetical effect that can never be observed in an actual experiment? Not quite. If the absolute truth is unattainable, then it can at least be approached! In other words, if Eqns (18) cannot be solved exactly, then one may try to find their approximate solution.

The previous analysis shows that the less strong restrictions for ε'' to observe the anomalous absorption are imposed in the vicinity of the dipole resonance. Then, a good material for a subwavelength particle to observe the anomalous absorption should have $\varepsilon' \approx -2$ and a small ε''. Such properties are exhibited, for example, by aluminum. It has

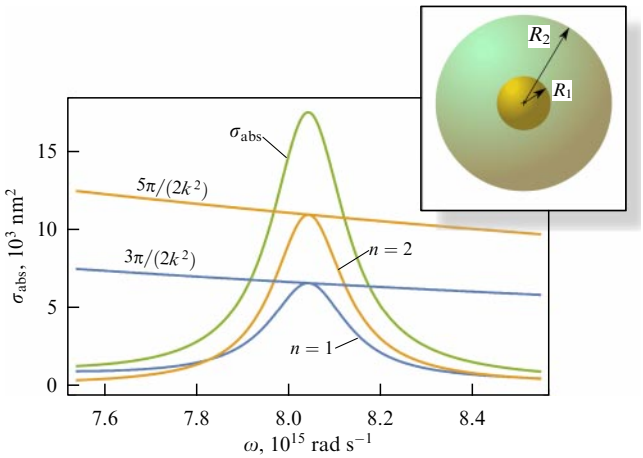

Figure 5. Absorption partial cross-section lines for electric dipole ($n = 1$) and quadrupole ($n = 2$) modes, as well as total absorption cross-section of the particle σ_{abs}, as functions of the frequency of an incident wave. Double-anomalous absorption by a particle with a gold core and a nonabsorbing dielectric shell (schematically depicted in the insert). Remaining parameters of the problem are fixed and equal to their resonant values [65, supplementary material]. Straight lines correspond to the maximal possible values of absorption partial cross-sections: $(2n + 1)\pi/(2k^2)$.

ε', monotonically decreasing from -0.51 at $\lambda = 100$ nm to -5.28 at $\lambda = 200$ nm, and ε'', monotonically increasing in the same range from 0.05 to 0.56. Notably, $\varepsilon'' = 0.16$ at $\varepsilon' = -2.00$ [69]. Accordingly, in Ref. [31], calculations were made of the absorption cross-section of an aluminum spherical particle upon its irradiation in a vacuum by a linearly polarized electromagnetic wave with cyclic frequency ω. The calculations were carried out based on the exact Mie solution with the actual experimental dependence $\varepsilon(\omega)$ for aluminum [69]. Its dependence on R was also taken into account through the contribution of collisions of free electrons with the particle's surface to the total collision frequency at $2R < \tau v_F$, where v_F stands for the free electrons' Fermi velocity and τ is the mean free time for electron–phonon collisions. Figure 4 shows the results of these calculations. Note the well-pronounced inverted hierarchy of resonances.

According to Fig. 4, the maximal dipole absorption is reached at $R \approx 11.8$ nm and the wavelength $\lambda \approx 152.8$ nm. The absorption cross-section is equal to 2.74×10^3 nm^2. Calculations using the formula $\sigma^{(a)}_{n,\,\mathrm{sca},\,\max}/4$, which determines the absolute maximum of the partial cross-section upon anomalous absorption, gives 2.79×10^3 nm^2, the difference between these two values is only in the third digit. Note also that the value of the geometric equatorial section of the sphere, πR^2, for this value of R is 0.44×10^3 nm^2. The absorption cross-section is 6.22 times more than this value: convincing evidence of the funnel effect [27].

Now, let us discuss which new peculiarities the problem acquires in the case of the mentioned multilayered particles. For the sake of simplicity, we limit ourselves only to core–shell particles, where a concentric shell with an outer radius of R_2 is located around a spherical core of radius R_1; see the insert in Fig. 5. Since the anomalous absorption conditions $\mathrm{Re}\, a_n = 1/2$, $\mathrm{Im}\, a_n = 0$ are formulated in terms of the scattering coefficients a_n solely and do not require their explicit dependence on the problem parameters, they remain the same for any spherically symmetric dependence $\varepsilon(r)$, i.e., do not formally change for a core-shell particle. ‡ However, the scattering coefficients now depend on a larger number of parameters. This gives us additional degrees of freedom that can be used to fulfill these conditions.

As an example, we consider the case of a core made of a material with a strong dispersion and a nonabsorbing shell, for which the dependence of ε on the problem parameters may be ignored. Then, instead of Eqns (18), we get the following equations:

$$\begin{aligned} &\mathrm{Re}\left[a_n\left(\frac{R_1\omega}{c}, \frac{R_2\omega}{c}, \varepsilon_1\left(\omega, R_1, R_2\right), \varepsilon_2\right)\right] = \frac{1}{2}\,, \\ &\mathrm{Im}\left[a_n\left(\frac{R_1\omega}{c}, \frac{R_2\omega}{c}, \varepsilon_1\left(\omega, R_1, R_2\right), \varepsilon_2\right)\right] = 0\,, \end{aligned} \tag{19}$$

where indices 1 and 2 refer to the core and shell, respectively, and $\varepsilon_2 = \mathrm{const}$ ($\mathrm{Im}\,\varepsilon_2 = 0$). We now have two conditions for four parameters: $R_{1,2}$, ε_2, and ω. This makes it possible either to select the values of the parameters to observe anomalous absorption in the desired area or to require that the resonant values of the parameters hold simultaneously for two different values of n. In the latter case, the particle behaves like a 'super-absorber', since its full absorption cross-section, which now includes two maximal partial ones, will significantly exceed the absolute upper limit existing for each of these partial modes separately. It is important to emphasize that the absorption occurs solely within the core. No energy release happens in the shell. The dielectric shell only causes the metal core to absorb the incident radiation more efficiently. Note that such a mechanism for designing a super-absorbing particle is quite similar to the one for a 'super-scattering' particle, discussed in Ref. [46].

Of course, as in the case of a homogeneous particle, the resulting equations may not always be solvable. However, the presence of free parameters makes the problem of absorption maximization for a layered particle much more flexible than it is in a spatially uniform case. In particular, the calculations presented in the supplementary material to publication [65] show that, for a particle with a metal core (gold) and a nondissipative dielectric shell, the complete overlap of the lines associated with the excitation of the ideal anomalous absorption in the dipole and quadrupole modes occurs at the following values of the problem parameters: $R_1 = 6.18$ nm, $R_2 = 31.04$ nm, $\varepsilon_2 = 3.55$, and $\omega = 8.04 \times 10^{15}$ rad s^{-1}, corresponding to the effect of UV radiation on a nanoparticle; see also Fig. 5.

Regarding experimental evidence for the results discussed here, despite the apparent importance of the problem both from the academic and practical (plenty of possible applications) points of view, reliable experiments in the optical range in which the anomalous scattering and/or absorption properties discussed here are confirmed (or refuted) are unknown to the authors. We hope that this review may stimulate such experiments.

5. Fano resonances

5.1 History of the question

We now move to another important type of resonance: Fano resonances, named after an Enrico Fermi's disciple Ugo Fano. First, let us briefly dwell on their story, since it is both

‡ *Authors' reformulated this sentence in English proof.*

entertaining and instructive. Apparently, Fano resonances were first observed in 1902 by Robert Wood when studying the diffraction of light on a reflecting diffraction grating (Wood's anomalies) [70], and their first explanation was given in 1907 by Lord Rayleigh [71]. What does Fano have to do with it? Here is what he has to do with it.

In 1935, Hans Beutler discovered in the spectrum of noble gases absorption lines of an unusual asymmetric form [72]. Surprisedly, they were observed in the region of the continuous spectrum, where no absorption lines should have been at all. Enrico Fermi, who then was a professor at the University of Rome La Sapienza, suggested explaining these experiments to his group, known as the 'via Panisperna boys' and named after the Institute of Physics located in Rome on the street with this name. There is now an excellent small cozy restaurant with the same name: Ragazzi di via Panisperna. The group consisted of a few junior scientists. There were Emilio Gino Segre, Bruno Pontecorvo, Ettore Majorana, and the very young 23-year-old Ugo Fano. All of them subsequently gained world fame.

However, it was just Ugo Fano who brilliantly tackled the problem posed by Fermi. It is worth mentioning that the complete solution to this problem was found in the archive remaining after Fermi's death. Fermi obtained it before or just after he posed the problem to the via Panisperna boys. However, when Fano completed his calculations and asked Fermi whether it was possible to start writing a joint paper, Fermi replied that it was; however, it was not to be a joint paper, but one attributed to Fano alone: ''You did everything yourself. It is enough just to put my name in the acknowledgment.'' Fano's article [73] was published in the same 1935 in the Italian journal *Nuovo Cimento* in Italian and... was overlooked by the community. To date, there are practically no citations of this paper.

Years went by. Destiny brought both scientists to the United States, where, in 1954, at the age of 53, Fermi passed away of stomach cancer. In 1961, Fano returned to his old work and published an extended version of it, this time in English in *Physical Review* [74]. In this article, Fano applied the formalism of delta functions, which made the work much more elegant.

Today, it is one of the most cited works ever published in all issues of *Physical Review*. What led to such stunning success of paper [74], while publication [73] is wholly forgotten? Fano himself writes the following in this regard [75]: ''The paper appears to owe its success to accidental circumstances, such as the timing of its publication and some successful features of its formulation.''

In our opinion, the first half of this phrase is not valid, but the second contains the keywords — there is nothing accidental in the article's success. It is not enough to get an outstanding result. This result must be understood and perceived by colleagues. To this end, it must be successfully formulated and also made public precisely at the time when it is in need. Furthermore, this must be done in the right place and in a language understandable to the international community. More detailed coverage of this story can be found in publications [76, 77].

5.2 Origin of Fano resonances and their description

It is high time to return from the history of the question to the discussion of its essence. What is it, and why was Fano's work, in such high demand in our time, overlooked in 1935?

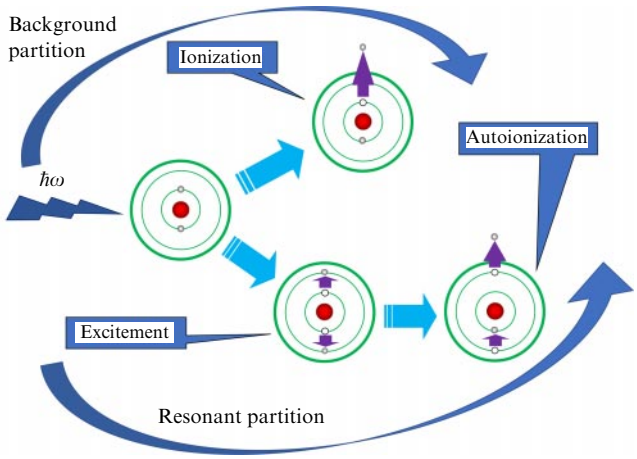

Figure 6. Two possibilities for photoionization of a helium atom. See main text for details.

Let us start with Beutler's experiments. For certainty, we will talk about the photoionization of an atom of helium. The corresponding qualitative picture is shown in Fig. 6. Being scattered by a helium atom, a photon may be absorbed by one of two valence electrons. If the photon energy is greater than the ionization potential, this electron acquires enough energy to leave the atom, and the latter becomes a positively charged ion. This photoionization process is well known to any student. Its probability weakly depends on the photon frequency, provided the frequency is greater than the ionization threshold. We will call such scattering background.

However, there is another possibility. If the photon energy is precisely equal to the sum of the excitation energies of both valence electrons, but at the same time, less than twice the ionization potential, then the absorption of the photon can lead not to knocking out one electron from the atom, but to the excitation of two electrons at once. At the same time, both of them remain bound. Then, the energy exchange between the two excited electrons begins. Since the excited electrons very poorly interact with each other, the energy exchange between them is slow (of course, in terms of the atomic time scale), and the atom lives in such an excited state for a long time. Nonetheless, this state cannot last forever. In the end, one of the electrons gives its energy to the other and relaxes into the ground state, while the other one acquires energy exceeding the ionization potential and leaves the atom. The probability of such a process (called autoionization) should decrease sharply when the photon energy departures from the value precisely equal the total energy of the two excited electrons. A process exhibiting a sharp, well-pronounced maximum in the dependence of the amplitude of the output on the frequency of the input is resonant. Therefore, it is also natural to call scattering leading to autoionization resonant.

As is known in quantum mechanics, if two different paths connect a given initial state (a photon scattered by a neutral atom) and the same final state (an ionized atom and a free electron), each of the paths is characterized by its own wave function. The complete wave function of the system is a linear superposition of these wave functions. The superposition leads to interference. Depending on the difference between their phases, the interference of two waves can give either a mutual gain (constructive interference) or suppression, up to total compensation (destructive interference).

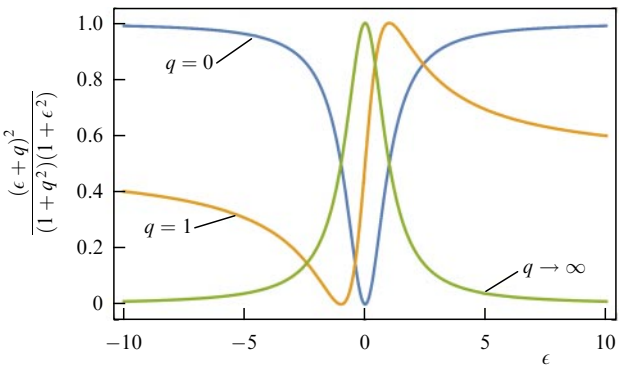

Figure 7. Fano profiles at different values of q (indicated in the figure). To bring all profiles to the same scale, the normalization constant in Eqn (20) is selected equal to $1/(1+q^2)$. Note that at $q=1$ the profile changes sharply and almost linearly between its minimum and maximum points.

This was the basis for Fano's explanation of Beutler's experiments. Specific calculations led him to a simple formula describing the shape of the line in this case:

$$\sigma = \text{const}\ \frac{(\epsilon+q)^2}{\epsilon^2+1}\,. \tag{20}$$

Here, ϵ is the normalized photon energy (not to be confused with permittivity ε), and $q=\text{const}$ designates the so-called Fano parameter, often called the asymmetry parameter of the lineshape.

It would seem that expression (20) is only slightly different from a Lorentzian due to the appearance of ϵ in the numerator. In fact, this is quite a distinct difference. In addition to breaking the mirror symmetry of the lineshape relative to the point $\epsilon=0$, now $\sigma(\epsilon)$ becomes zero at $\epsilon=-q$, which is obviously the result of destructive interference. Lines $\sigma(\epsilon)$ at different values of q are shown in Fig. 7. At $q\to\infty$, Fano's profile transforms into a regular Lorentzian.

Let us summarize some of the above results. It may be said that Fano resonances occur owing to a double reaction of the system to an input signal, generating not one but two output signals interfering with each other. This formulation clarifies that the Fano resonances are quite a general property of dynamic systems, which a broad class of quantum and classical problems may exhibit. Moreover, even the wave nature of the interfering signals is not necessary. Instead of wave interference, it is possible to consider a superposition of oscillations in discrete systems. A large number of specific examples of Fano resonances in various systems and their detailed discussion can be found, for example, in reviews [19, 78] and the references therein.

However, the highlighted possibility of a broad class of various systems exhibiting Fano resonances is not the only explanation for the dizzying success of Fano's 1961 publication. In the time that passed from 1935 to 1961 (and even more so from 1961 to the present day), the accuracy of measurements had increased drastically. More and more precise sensors are needed. Fano's resonances are specifically helpful to respond to this challenge. Indeed, Fig. 7 shows that, at q of the order of unity in the range of ϵ values lying between the points of the minimum and maximum of the Fano profile, this profile is almost linear and, moreover, has a steep slope. This means that, in this area, a slight change in the input signal (ϵ) leads to a significant (and practically linear!) change in the output signal. A sensor with such properties is a big dream of any expert involved in precise measurements.

Furthermore, this is not yet all. If σ in Eqn (20) means the cross-section of light scattering, then at the point $\epsilon=-q$ it becomes zero. In other words, such a particle does not scatter anything, i.e., does not perturb the fields of the incident wave. If so, it is invisible to an external observer. Significantly, simultaneously, the field inside the particle is in no way zero; see below. Furthermore, this field may be considerably larger than that in the incident wave. However, this large field is confined in the particle and does not leak out of it [79].

There is an unbelievable case: a strong oscillating electromagnetic field inside a particle causes oscillations of free and/or bound charges, but these oscillating charges do not emit electromagnetic waves! It would seem that this cannot be, "because this never can be" — but it can. Such excitations (they are called anapole — from Greek, where *an* is a prefix meaning negation; *polos* means pole, i.e., no poles) were introduced by Ya B Zeldovich to explain the parity violation in the atomic nucleus in weak interactions [80]. In the problems of light scattering by nanoobjects, anapoles were considered in [81] and in a large number of later publications [37, 38, 82–88].

The existence of such nonradiating excitations opens up vast possibilities for creating ultra-precise sensors capable of measuring electromagnetic fields without distorting them by the sensors themselves; a new generation of information recording, reading, and processing systems; new materials; etc. However, we are not in a position to discuss here applications of this effect. Our goal is to answer the question of what Fano resonances have to do with the topic of the present review. Let us try to figure it out.

5.3 Fano resonances and longitudinal electromagnetic modes

A distinctive feature of Fano resonances in light scattering by a subwavelength particle should be the vanishing of a partial scattering cross-section due to the destructive interference of two modes with the same value of n and the same nature (i.e., both either electric or magnetic). The same n and nature are required because, otherwise, the modes will have a different angular dependence of the scattered radiation (see [1–4], also the Appendix), and their interference in principle cannot result in mutual compensation of the radiation in all directions at once.

It would seem that all previous consideration suggests that, for small metal particles, such pairs of modes do not exist. Indeed, as shown in Eqns (2), (4), a_n never goes to zero unless $\varepsilon\neq 1$. The case of $\varepsilon=1$ is not of interest to us, since, when this condition is met, the particle optically becomes identical to the ambient medium and ceases to exist as a wave-scattering obstacle. From all of this, it would seem that small metal particles cannot, in principle, exhibit Fano resonances.

In fact, this is not quite true: in addition to $\varepsilon=1$ in electrodynamics, there is another singled out value of ε, namely $\varepsilon=0$. At this value of permittivity, the electric induction vector **D** equals zero identically. Then, it becomes possible to excite longitudinal electromagnetic modes, for the accurate description of which it is necessary to take into account the effects of spatial dispersion [23]. The dispersion law for the longitudinal modes have the form

$$\varepsilon_{\parallel}(k_{\parallel},\omega)=0\,, \tag{21}$$

while transverse modes are described by the usual dispersion relation

$$k_{\perp}^2 = \varepsilon_{\perp}(\omega)\,\frac{\omega^2}{c^2}\,. \tag{22}$$

Of course, longitudinal modes may exist only inside the particle — where permittivity is close to zero. At the same time, $\mathbf{D} = 0$ converts one of Maxwell's equations to $[\nabla \times \mathbf{H}] = 0$. Another of Maxwell's equations states that $(\nabla \mathbf{H}) = 0$. A vector field satisfying two such equations simultaneously is a constant. To fulfill the boundary conditions on the surface of the sphere, the constant must be assigned a zero value.

Thus, the longitudinal oscillations of the field are not electromagnetic but solely electric: the magnetic field is not excited. If so, then the Poynting vector of the oscillations is identically equal to zero. Therefore, due to the continuity of the energy flow through the surface of the particle, the longitudinal modes are nonemitting and cannot contribute to interference. However, through the boundary conditions on the sphere's surface, these modes are coupled with conventional transverse field oscillations. As a result, the conventional Mie solution is modified.

A study of the problem, which takes into account these modifications, is presented in publications [89, 90] and, with a focus on the Fano resonances, specifically, in Ref. [79]. It is shown there that, in small metal particles, the longitudinal modes give rise to the emergence of a cascade of Fano resonances located in the vicinity of the point $\varepsilon_{\perp}(\omega) = 0$. Unfortunately, these resonances can hardly be of practical interest for the optics of nano-objects, since dissipative damping extremely strongly suppresses them, and at values of the problem parameters corresponding to actual metals, their effect on scattering processes is negligible.

5.4 Directional Fano resonances

5.4.1 Theory. However, is the possibility of excitation of Fano resonances upon light scattering by subwavelength particles exhausted in the above discussion? Let us return to the nature of these resonances, which requires having at least two interfering scattered waves. At the same time, for destructive interference to occur, these waves must simultaneously satisfy two conditions: having equal amplitudes and opposite phases.

We turn again to expression (2) for the scattering coefficients. As already noted, in the nondissipative limit, the functions F_n and G_n are purely real. Moreover, on the wings of the resonant line, when $|G_n| \gg |F_n|$, $a_n \approx -\mathrm{i}F_n/G_n$, i.e., it has an almost purely imaginary value.

Furthermore, by definition, function G becomes zero at the resonance points. Then, when ε passes the resonance point, G changes sign; see Eqn (5). In other words, the passage of the resonance gives rise to a phase shift of π for the corresponding scattering coefficient — a fact well known from oscillation theory.

With this in mind, consider Fig. 1. As stressed above, though the figure corresponds to $x \sim 1$, there is no qualitative difference between it and a similar figure at $x \ll 1$. The figure shows a relatively wide dipole resonance line, on a wing of which there is an intense narrow quadrupole resonance line. At the same time, at $x \ll 1$, the condition $\varepsilon \approx -3/2$ must be met at the point of quadrupole resonance. Then, in this area, the partial efficiency of dipole scattering is of the order of $x^2 \ll 1$, and the partial efficiency of the quadrupole resonance in the maximum is of the order of $1/x^2 \gg 1$; see Eqns (2)–(5), (10).

From the above, it follows that the efficiencies of the dipole and quadrupole scattering (and, therefore, the corresponding fields of the partial waves) are equal at two points lying on either side of the point of the maximum of the quadrupole resonance. At the same time, at the points of equality, the amplitudes of the partial modes are still much less than the maximal value of the amplitude of the quadrupole mode at the resonance point. In other words, both points of the equal amplitudes lie on the wings of the quadrupole resonance line. The quadrupole resonance line itself lies on the wing of the dipole line. Then, taking into account what was said in the preceding paragraph, we conclude that, in one of the points of equality, the amplitudes of the scattering coefficients a_1 and a_2 are equal, and their phases are opposite. That is to say, both destructive interference conditions inevitably will be met in the vicinity of one of these points. However, such destructive interference is qualitatively different from the case discussed earlier.

In conventional Fano resonances, the interfering modes have the same angular dependence of scattered radiation. Therefore, equal amplitudes and opposite phases of these modes ensure that the scattered radiation intensity goes to zero in all directions at once. That is to say, the corresponding integral scattering cross-section vanishes. Now, we are talking about the interference of the modes with different values of n. As already noted, the angular dependence of the scattered field for such modes is also different. Therefore, turning to zero the intensity of the scattered radiation in all directions at once due to their destructive interference is fundamentally impossible. In this case, the complete mutual cancellation of the scattered waves may be achieved just along a specific direction; that is, only the contribution of these modes to the differential scattering cross-section may vanish. It is essential that every direction has its own destructive interference frequency.

Thus, due to the interference of the waves emitted by different multipoles, the intensity of the radiation scattered along a given fixed direction as a function of the frequency of the incident wave may exhibit an asymmetric Fano profile. At the same time, according to Eqns (3), (8), the integral scattering cross-section is described by a symmetric Lorentzian [91].

In order to quantify these effects, we have to consider the interference of fields emitted by different multipoles. This is easy to do by taking advantage of the known expression for the intensity of radiation scattered along a given direction. If one selects a spherical coordinate frame whose center coincides with the center of the scattering sphere, then, for a plane linearly polarized incident wave propagating along the positive direction of the z-axis, with the oscillation plane of the $\mathbf{E}$ vector coinciding with the xz plane, the intensity of the radiation scattered along a given direction has in the far wave zone the following components of vector $\mathbf{E}$ [4]:

$$|E_{\theta}^{\mathrm{sca}}|^2 = I_{\parallel}\cos^2\varphi, \quad |E_{\varphi}^{\mathrm{sca}}|^2 = I_{\perp}\sin^2\varphi\,, \tag{23}$$

where θ and φ stand for the polar and azimuthal angles, respectively, and $I_{\parallel}$ and $I_{\perp}$ are determined by the corresponding multipole expansion. According to what was said above, in the vicinity of the quadrupole resonance ($\varepsilon = -3/2$) in this expansion, it is enough for us to keep only the dipole and

quadrupole terms. At the same time, in the dipole term, in the leading approximation, we can set $\varepsilon = -3/2$, and in the quadrupole term use formula (8).

As a result, dropping a common multiplier for $I_{\parallel,\perp}$, we get [91]

$$I_{\parallel}^{(s)} \propto \left| \mathrm{i}x^3 \cos\theta + \frac{x^5 \cos(2\theta)}{2(x^5 - 12\mathrm{i}\delta\varepsilon)} \right|^2, \tag{24}$$

$$I_{\perp}^{(s)} \propto \left| \mathrm{i}x^3 + \frac{x^5 \cos\theta}{2(x^5 - 12\mathrm{i}\delta\varepsilon)} \right|^2. \tag{25}$$

Note that, in full accordance with the qualitative picture discussed above, the resulting expressions have two characteristic scales. One of them describes a narrow resonant peak associated with the quadrupole resonance. Its width is determined by Eqn (8) for γ_n at $n = 2$ and on the ε axis is equal to $x^5/6$. The other one, much wider, is defined by the position of the destructive resonance point and is slightly different for the two polarizations of the scattered light: $\delta\varepsilon_{\parallel} = -x^2 \cos(2\theta)/24\cos\theta$ and $\delta\varepsilon_{\perp} = -x^2\cos\theta/24$ (we remind the reader that here $\delta\varepsilon$ stands for the departure of ε from the center of the quadrupole resonance line).

It is noteworthy that, according to Eqns (24), (25), intensities $I_{\parallel,\perp}$ depend on θ but not on φ. In other words, they remain constant on the surface of a cone with an axis coinciding with the z-axis and a fixed apex angle but change with variations in the apex angle. We also emphasize that the destructive interference points can be situated on different sides of the point $\delta\varepsilon = 0$; their specific location depends on the value of θ and the polarization of the scattered radiation. Thus, the directional Fano resonances are a powerful tool to create various scattered radiation patterns, significantly suppressing scattering along almost any desired direction only by adequately selecting the frequency of the incident wave.

That is, in theory. What in this case does "its majesty experiment" say? We should stress that, despite the ideological simplicity, technically, experiments devoted to the issues discussed in this review are usually challenging, since they require carrying out subtle, precise measurements at the nanoscale. Apparently, for this reason, even though theoretically directional Fano resonances were discussed even in 2008 [91, 92], experimental evidence of them was revealed only eight years later [93].

5.4.2 Experiment. Let us turn to a brief discussion of these experiments. First of all, note that the directional Fano resonances are realized when a wing of a relatively broad line of one multipole overlaps with a narrow resonance line of a multipole with another (usually higher) multipolarity. At the same time, these two multipoles should make an overwhelming contribution to the integral scattering cross-section.

Further, the scattering diagram of each multipole is determined by the type of the problem's eigenfunctions. These eigenfunctions depend on the problem's symmetry but do not depend on the material properties of the scattering particle. The latter affects only and exclusively the values of the scattering coefficients.

It is clear from the preceding that the negativity of $\mathrm{Re}\,\varepsilon$ for the scattering particle is not necessary to observe directional Fano resonances. Dielectrics with $\mathrm{Re}\,\varepsilon > 0$ can also exhibit such resonances, provided that the spectral dependence of their resonance lines satisfies the properties noted above.

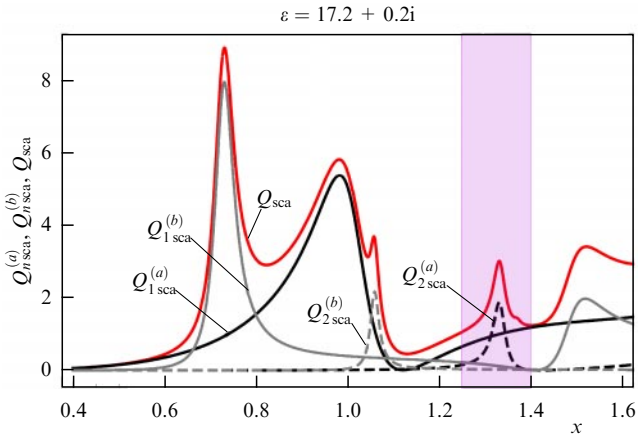

Figure 8. Integral scattering efficiency Q_{sca} and partial efficiencies of the first four multipoles: electric dipole ($Q_{1\,\mathrm{sca}}^{(a)}$), magnetic dipole ($Q_{1\,\mathrm{sca}}^{(b)}$), electric quadruple ($Q_{2\,\mathrm{sca}}^{(a)}$), and magnetic quadruple ($Q_{2\,\mathrm{sca}}^{(b)}$) for a spherical particle with $\varepsilon = 17.2 + 0.2\mathrm{i}$ as functions of its size parameter. Highlighted area indicates where directional Fano resonances can be observed.

Another essential point to be made is the scale invariance of Maxwell's equations: suppose one changes the geometric dimensions of the problem simultaneously with the radiation wavelength so that their ratio remains fixed, and the dielectric constant remains unchanged. In this case, the scattering problem will be identical to the original one. This makes it possible to mimic light scattering by a nanoparticle, studying the equivalent problem of scattering radiation with a significantly larger wavelength by a macroscopic object of the same shape.

The authors of Ref. [93] employed this approach for the experimental study of directional Fano resonances. In particular, a sphere 18 mm in diameter was made of special ceramics. The sphere's permittivity in the centimeter range was $\varepsilon \approx 17.2 + 0.2\mathrm{i}$, which approximately corresponded to the dielectric constant of widespread semiconductor materials (Si, Ge, GaAs, GaP) in the optical and near IR ranges. The integral scattering efficiency of such a sphere and the partial efficiencies of its dipole and quadrupole modes are shown in Fig. 8 as functions of its size parameter. It is seen that, in the region $1.25 < x < 1.40$, the electric dipole and quadrupole modes make the overwhelming contribution to the total scattering efficiency, and that in this region the conditions highlighted above to observe the directional Fano resonances due to interference of the radiation of these two partial modes are fulfilled.

To study the angular and frequency dependences of the scattered radiation, a ceramic sphere was placed in a special chamber with a nonreflective coating on its walls, where it was irradiated with a plane linearly polarized electromagnetic wave in the centimeter range. A special antenna received the radiation scattered by the sphere in a given direction. The extinction cross-section was determined based on the optical theorem [3, 4] by measuring the amplitude and phase of the scattered forward wave at two independent radiation polarizations.

We will not dwell here on the details of this experiment, that is quite technically complex. The interested reader can find them in the original publication [93] and references therein. As an example, graphs of intensity $I_{\perp}$ scattered along the direction determined by the value of the polar angle θ obtained in this study as functions of the wavelength

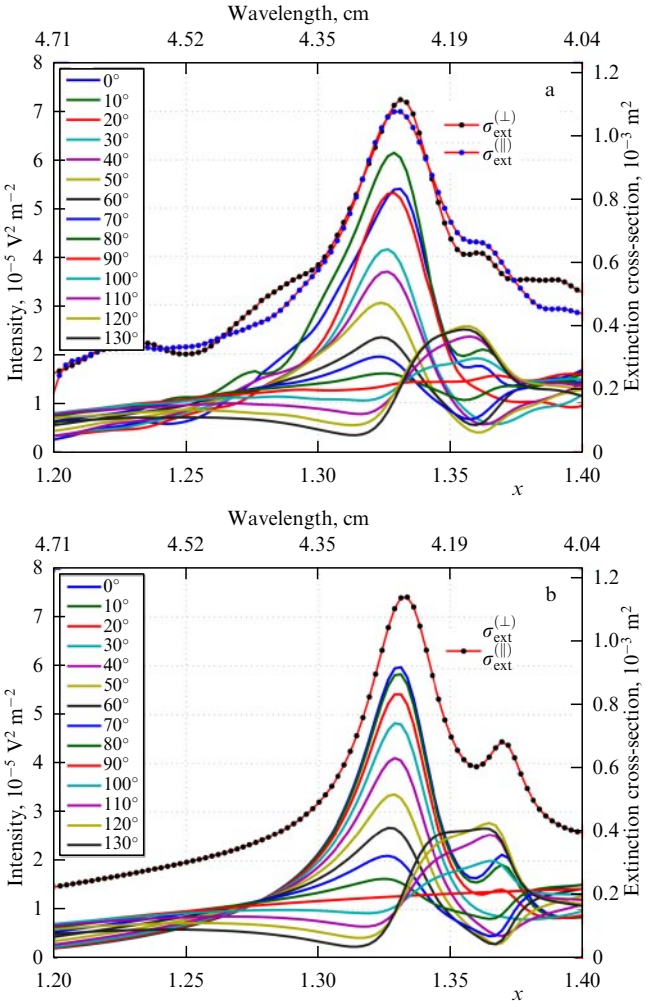

Figure 9. Scattering intensity $I_\perp$ along different directions, determined by values of polar angle θ (indicated in the insert), as a function of radiation wavelength [93]. Ceramic sphere with a diameter of 18 mm. In the specified range, dispersion dependency $\varepsilon(\omega)$ can be ignored: it may be supposed that $\varepsilon(\omega) \approx 17.2 + 0.2\mathrm{i}$. (a) — measurement, (b) — calculations by Mie's formulas. See main text for details.

of the incident radiation are presented in Fig. 9a. Figure 9b shows the same dependence calculated based on the exact Mie solution. We emphasize that not a single fitting parameter was used in this approach. Note also that, when the values of θ pass through the point $\theta = 90°$, the mutual sequence of the points of the minima and maxima of the profiles $I_\perp(x)$ is inverted; see Eqn (25). We draw the reader's attention to the fact that, at $\theta > 90°$, the local minima of the directional scattering are located at almost the same value of x, which corresponds to the local maximum of the integral extinction cross-section. This result would be difficult to understand outside the framework of the ideas discussed above.

6. Conclusions

Let us summarize some results. In this review, we have discussed only a few new and, from our point of view, rather unusual aspects of the old problem of light scattering by small particles. Keeping the scope of the review within reasonable limits and at the same time being able to discuss in detail the physics of the underlying processes and phenomena, we have been forced to sacrifice many vital issues and applications associated with them. Such issues excluded from the discussion primarily include the problems of light scattering by particles of complex shape (discs; ellipsoids, including highly elongated or strongly flattened; toroidal particles — 'doughnuts'; pyramids and other polyhedrons; etc.), clusters of several nanoparticles — 'metamolecules', as well as metamaterials and metasurfaces. Their discussion is presented in a large number of both original publications (experimental and theoretical), reviews, and monographs; see, for example, Refs [18, 20, 94–100], to which we refer the interested reader.

In our view, this selection of the material is justified, since a deep understanding of the physics of relatively simple cases considered in the review helps to create a general picture of the phenomenon characteristic of more complex problems. Moreover, in some cases, the Mie solution for a sphere discussed in the review can be employed as a basic approximation to describe more complex cases (a sphere on a substrate, metamolecules, etc.) employing perturbation theory.

As for applications of these effects, their spectrum is vast. In particular, the resonant local enhancement of electromagnetic field makes it possible to create areas of a subwavelength size for selective powerful electromagnetic impact on biological tissues, which opens up fundamentally new opportunities in genetic engineering and nanosurgery at the cellular level, the treatment of oncological diseases, the creation of new drugs, etc.

The same properties, complemented by the ability to switch between different states and control scattering patterns smoothly, can be widely used in the development of new methods for transmitting, recording, and the ultra-high density storage of information, as well as ultra-fast information processing, including the creation of fundamentally new multi-functional ultra-close-packed elements for integrated optics, which can be used, for example, in the design of high-performance optical computers built on the principles of fiber optics. These properties can also serve as a basis for a breakthrough in visualizing objects with ultra-high spatial and temporal resolution and ultra-high resolution spectroscopy.

In the review, we ultimately did not address the discussion of various nonlinear phenomena. However, the funnel effect noted above indicates the possibility of creating regions with a huge electromagnetic energy density at very moderate values of the intensity of the incident radiation. Suppose the scattering particle is immersed in a nonlinear medium (or has nonlinear properties itself). In this case, the presence of such areas should give rise to a great increase in the efficiency of high harmonic generation, which opens up prospects for creating, e.g., a new generation of biological and medical markers. Such markers will allow obtaining a response signal with ultra-high (subcellular) spatial resolution at record low intensity of the probing pulse and a corresponding reduction in its side-effects on the biologically examined tissues.

These are just a few examples. The list can easily go on. We hope that this review will be helpful in this kind of research.

Note that, for the time being, due to difficulties in getting materials with the necessary properties in the optical frequency range, some of the effects discussed in the review do not have direct experimental evidence. These difficulties are largely overcome in the radio band. In addition, the discussed results are pretty easily transferred to the scattering of waves of a different nature, for example, acoustic, where the material restrictions on the properties of both the medium

through which the waves propagate and the objects scattering these waves have entirely different frameworks.

As for the observation of the discussed effects precisely in light scattering, the fantastic successes achieved recently in the creation of metamaterials with predetermined properties make it possible to hope that any restrictions imposed on the properties of the matter, and not related to the manifestation of the fundamental laws of physics, can be eliminated. This gives the theoretical research discussed in this review very practical meaning.

The authors are grateful to A S Sigov for the careful reading of the manuscript and valuable remarks contributing to its improvement.

The review was written with the financial support of the Russian Foundation for Basic Research (project no. 19-12-50016); the Russian Science Foundation (project no. 19-72-30012), within the framework of which all original calculations given in this publication were performed; and the Russian Foundation for Basic Research (project no. 20-02-00086) for visualization of the results of numerical calculations and computer graphics.

7. Appendix. Mathematical supplement

A. Exact Mie solution for a sphere

Here are the main results of Mie's theory for reference. We consider the scattering of a plane linearly polarized electromagnetic wave with a cyclic frequency ω and a wave vector $\mathbf{k}$ oriented along the axis z by a homogeneous sphere of radius R, the center of which is placed at the origin of the spherical coordinate frame. Under the assumptions made, the electric field of the incident wave is described by the formula

$$\mathbf{E}^{\text{inc}} = \mathbf{E}_0 \exp\left[\mathrm{i}(kz - \omega t)\right], \tag{26}$$

where the vector $\mathbf{E}$ is directed along the axis x. It is convenient to introduce the dimensionless fields $\mathcal{E} = E/E_0$ and $\mathcal{H} = H/H_0$. Here, $H_0 = E_0\sqrt{\varepsilon_{\text{out}}/\mu_{\text{out}}}$ is the amplitude of magnetic field in the incident wave. To make the problem formulation more general, it is no longer assumed that the magnetic permeability is identically equal to unity. Then, the expressions below may be used for magnetic particles as well. Of course, in this case, the relative refractive index of a sphere m should be considered equal to $m = \sqrt{\varepsilon_{\text{in}}\mu_{\text{in}}/(\varepsilon_{\text{out}}\mu_{\text{out}})}$.

Expanding the field of the incident wave in spherical harmonics, we present it as the following infinite series of partial waves [1, 3, 4]:

$$\begin{aligned}\mathcal{E}^{\text{inc}}_{r,\theta,\varphi} &= \exp(-\mathrm{i}\omega t)\sum_{n=1}^{\infty}\mathcal{E}^{\text{inc}\,(n)}_{r,\theta,\varphi};\\ \mathcal{H}^{\text{inc}}_{r,\theta,\varphi} &= \exp(-\mathrm{i}\omega t)\sum_{n=1}^{\infty}\mathcal{H}^{\text{inc}\,(n)}_{r,\theta,\varphi},\end{aligned} \tag{27}$$

where

$$\mathcal{E}^{\text{inc}\,(n)}_{r} = \mathrm{i}^{n-1}\,\frac{2n+1}{(kr)^2}\,\psi_n(kr)\pi_n(\theta)\sin\theta\cos\varphi, \tag{28}$$

$$\mathcal{E}^{\text{inc}\,(n)}_{\theta} = \mathrm{i}^{n}\,\frac{2n+1}{kr(n+1)n}\left[\psi_n(kr)\pi_n(\theta) - \mathrm{i}\psi_n'(kr)\tau_n(\theta)\right]\cos\varphi, \tag{29}$$

$$\mathcal{E}^{\text{inc}\,(n)}_{\varphi} = -\mathrm{i}^{n}\,\frac{2n+1}{kr(n+1)n}\left[\psi_n(kr)\tau_n(\theta) - \mathrm{i}\psi_n'(kr)\pi_n(\theta)\right]\sin\varphi, \tag{30}$$

$$\mathcal{H}^{\text{inc}\,(n)}_{r} = \mathrm{i}^{n-1}\,\frac{2n+1}{(kr)^2}\,\psi_n(kr)\pi_n(\theta)\sin\theta\sin\varphi, \tag{31}$$

$$\mathcal{H}^{\text{inc}\,(n)}_{\theta} = \mathrm{i}^{n}\,\frac{2n+1}{kr(n+1)n}\left[\psi_n(kr)\pi_n(\theta) - \mathrm{i}\psi_n'(kr)\tau_n(\theta)\right]\sin\varphi, \tag{32}$$

$$\mathcal{H}^{\text{inc}\,(n)}_{\varphi} = \mathrm{i}^{n}\,\frac{2n+1}{kr(n+1)n}\left[\psi_n(kr)\tau_n(\theta) - \mathrm{i}\psi_n'(kr)\pi_n(\theta)\right]\cos\varphi. \tag{33}$$

Here, θ and φ stand for the polar and azimuthal angle, respectively, the prime means the derivative with respect to the entire argument of a function, and the following notations are employed:

$$\psi_n(z) = \sqrt{\frac{\pi z}{2}}\,J_{n+1/2}(z), \quad \pi_n(\theta) = \frac{P_n^1(\cos\theta)}{\sin\theta}, \tag{34}$$

$$\tau_n(\theta) = \frac{\mathrm{d}P_n^1(\cos\theta)}{\mathrm{d}\theta}, \quad P_n^m(z) = (1-z^2)^{m/2}\,\frac{\mathrm{d}^m P_n(z)}{\mathrm{d}z^m}, \tag{35}$$

where $J_{n+1/2}(z)$ is the Bessel function, and $P_n(z)$ is the Legendre polynomials.[‡] The functions $\psi_n(z)$ and $\xi_n(z)$ introduced below are often called Riccati–Bessel functions.

With the chosen problem formulation, namely the scattering by a spherical particle of a plane electromagnetic wave, Eqn (26), its expansion in spherical harmonics (35) includes only modes with $m = 1$ (here, m is the upper index in $P_n^m(z)$, not to be confused with the refractive index). In other cases, for example, when a sphere is irradiated by a focused or singular beam, generally speaking, all harmonics with $-n \leqslant m \leqslant n$ must be taken into account [101–103]. However, since the set of plane wave functions is complete, and any arbitrary electromagnetic wave can be represented as their superposition, we will not consider such cases, discussing just the scattering of a plane monochromatic wave.

The scattered radiation field (index 'sca') and the field inside the particle (index 'in') are represented in series similar to Eqn (27), where the corresponding partial waves are determined by the expressions

$$\mathcal{E}^{\text{sca}\,(n)}_{r} = -\mathrm{i}^{n-1}\,\frac{2n+1}{(kr)^2}\,a_n\xi_n(kr)\pi_n(\theta)\sin\theta\cos\varphi, \tag{36}$$

$$\mathcal{E}^{\text{sca}\,(n)}_{\theta} = -\mathrm{i}^{n}\,\frac{2n+1}{kr(n+1)n} \times \left[b_n\xi_n(kr)\pi_n(\theta) - \mathrm{i}a_n\xi_n'(kr)\tau_n(\theta)\right]\cos\varphi, \tag{37}$$

$$\mathcal{E}^{\text{sca}\,(n)}_{\varphi} = \mathrm{i}^{n}\,\frac{2n+1}{kr(n+1)n} \times \left[b_n\xi_n(kr)\tau_n(\theta) - \mathrm{i}a_n\xi_n'(kr)\pi_n(\theta)\right]\sin\varphi, \tag{38}$$

$$\mathcal{H}^{\text{sca}\,(n)}_{r} = -\mathrm{i}^{n-1}\,\frac{2n+1}{(kr)^2}\,b_n\xi_n(kr)\pi_n(\theta)\sin\theta\sin\varphi, \tag{39}$$

[‡] Note that, sometimes on the r.h.s. of expression (35) for $P_n^m(z)$, the factor $(-1)^m$ is included. We do not do so. (*Authors' note to English proof.*)

$$\mathcal{H}_{\theta}^{\mathrm{sca}\,(n)} = -\mathrm{i}^{n}\frac{2n+1}{kr(n+1)n} \times \left[a_n\xi_n(kr)\pi_n(\theta) - \mathrm{i}b_n\xi_n'(kr)\tau_n(\theta)\right]\sin\varphi\,, \tag{40}$$

$$\mathcal{H}_{\varphi}^{\mathrm{sca}\,(n)} = -\mathrm{i}^{n}\frac{2n+1}{kr(n+1)n} \times \left[a_n\xi_n(kr)\tau_n(\theta) - \mathrm{i}b_n\xi_n'(kr)\pi_n(\theta)\right]\cos\varphi\,. \tag{41}$$

$$\mathcal{E}_{r}^{\mathrm{in}\,(n)} = \mathrm{i}^{n-1}\frac{2n+1}{(mkr)^2}\,d_n\psi_n(mkr)\pi_n(\theta)\sin\theta\cos\varphi\,, \tag{42}$$

$$\mathcal{E}_{\theta}^{\mathrm{in}\,(n)} = \mathrm{i}^{n}\frac{2n+1}{mkr(n+1)n} \times \left[c_n\psi_n(mkr)\pi_n(\theta) - \mathrm{i}d_n\psi_n'(mkr)\tau_n(\theta)\right]\cos\varphi\,, \tag{43}$$

$$\mathcal{E}_{\varphi}^{\mathrm{in}\,(n)} = -\mathrm{i}^{n}\frac{2n+1}{mkr(n+1)n} \times \left[c_n\psi_n(mkr)\tau_n(\theta) - \mathrm{i}d_n\psi_n'(mkr)\pi_n(\theta)\right]\sin\varphi\,, \tag{44}$$

$$\mathcal{H}_{r}^{\mathrm{in}\,(n)} = \mathrm{i}^{n-1}\frac{2n+1}{m(kr)^2}\,c_n\psi_n(mkr)\pi_n(\theta)\sin\theta\sin\varphi\,, \tag{45}$$

$$\mathcal{H}_{\theta}^{\mathrm{in}\,(n)} = \mathrm{i}^{n}\frac{2n+1}{kr(n+1)n} \times \left[d_n\psi_n(mkr)\pi_n(\theta) - \mathrm{i}c_n\psi_n'(mkr)\tau_n(\theta)\right]\sin\varphi\,, \tag{46}$$

$$\mathcal{H}_{\varphi}^{\mathrm{in}\,(n)} = \mathrm{i}^{n}\frac{2n+1}{kr(n+1)n} \times \left[d_n\psi_n(mkr)\tau_n(\theta) - \mathrm{i}c_n\psi_n'(mkr)\pi_n(\theta)\right]\cos\varphi\,. \tag{47}$$

Here, $\xi(z)$ is associated with the Hankel function of the first kind, $H_{\nu}^{(1)}$, as follows: $\xi_n(z) = \sqrt{\pi z/2}\,H_{n+1/2}^{(1)}(z)$, and the scattering coefficients a_n, b_n, c_n, and d_n are determined from the continuity condition of the tangential components of the fields **E** and **H** on the surface of the sphere, resulting in the following expressions:

$$a_n = \frac{m\psi_n(mx)\psi_n'(x) - \psi_n(x)\psi_n'(mx)}{m\psi_n(mx)\xi_n'(x) - \xi_n(x)\psi_n'(mx)}\,, \tag{48}$$

$$b_n = \frac{m\psi_n(x)\psi_n'(mx) - \psi_n(mx)\psi_n'(x)}{m\xi_n(x)\psi_n'(mx) - \psi_n(mx)\xi_n'(x)}\,, \tag{49}$$

$$c_n = -\frac{\mathrm{i}m}{m\xi_n(x)\psi_n'(mx) - \psi_n(mx)\xi_n'(x)}\,, \tag{50}$$

$$d_n = \frac{\mathrm{i}m}{m\psi_n(mx)\xi_n'(x) - \xi_n(x)\psi_n'(mx)} \tag{51}$$

(in Eqns (50), (51), we used the identity $\psi_n(x)\xi_n'(x) - \psi_n'(x)\xi_n(x) \equiv \mathrm{i}$ [104]).

Note that, as follows from the above expressions, the radial components of the fields of scattered partial spherical waves are not equal to zero. This means that these waves are not entirely transversal. They become transversal only asymptotically at $r \to \infty$, because the radial components decrease with an increase in r faster than the tangential ones.

Knowing the coordinate dependence of all components of the scattered field and calculating the vector product $[\mathbf{E} \times \mathbf{H}]$, one can obtain a Poynting vector profile, from which, in particular, Eqns (24), (25) follow. We are not going to do this here.

Note that a similar exact solution can be obtained for the scattering of a plane linearly polarized wave by an infinite circular cylinder. This can be done at arbitrary orientations of the cylinder axis relative to the wave vector of the incident wave and plane of its polarization. The difference between this and the problem for a sphere is that, in this case, the natural coordinate frame is cylindrical, and the expansion should be carried out not in spherical but in the cylindrical functions. However, the explicit form of such a solution is very cumbersome and will not be given here. It can be found, for example, in books [1, 3].

B. General properties of scattering coefficients

From expressions (36)–(41), (48), (49), it follows that the entire dependence of scattered radiation on the individual properties of a scattering particle is determined by the scattering coefficients a_n, b_n — all other expressions entering Eqns (36)–(41) are universal and remain the same for any spherical particles. All partial cross-sections are also expressed in terms of the scattering coefficients; see Eqns (3), (14). Similar claims are true when light is scattered by a cylinder. For this reason, the scattering coefficients play a fundamental role in the problem under consideration. Let us show that these coefficients have certain important universal properties following from the general features of the scattering problem and hidden in cumbersome expressions (48), (49) [26, 65].

To clarify these properties, we take advantage of the fact that the orthogonal modes included in the multipole expansion of the scattered field are the eigenfunctions of the corresponding boundary value problem. This means that none of them has projections on any other, and each can be excited independently. This claim is valid for the electric and magnetic modes with the same value of n, since they are not coupled through boundary conditions, and the scattering problem is linear.

Furthermore, note that formulas (3), (14) for partial cross-sections are directly derived from the orthogonality of the eigenfunctions of the problem and the optical theorem. The latter, in turn, is a direct consequence of the energy conservation law [1, 3, 4]. Therefore, the range of their applicability extends far beyond the exact Mie solution for a sphere.

Bearing this in mind, we now consider the excitation of such a single partial mode. The corresponding scattering coefficient is denoted by z_n, where z_n can represent both a_n and b_n. As usual, first, we discuss the nondissipative case ($\mathrm{Im}\,\varepsilon = 0$). In the absence of dissipation, all absorption partial cross-sections are identically equal to zero. Being applied to expression (14), this condition results in the equality $\mathrm{Re}\,z_n = |z_n|^2$. Representing the complex scattering coefficient as $z_n = z_n' + \mathrm{i}z_n''$, we make sure that this is equivalent to the condition $z_n' - z_n''^2 = z_n'^2 \geqslant 0$. Then, it immediately follows that $z_n' \geqslant z_n''^2 \geqslant 0$ and $z_n' \geqslant z_n'^2$, which, in turn, leads to the restriction $0 \leqslant z_n' \leqslant 1$. Finally, any positive number that does not exceed unity can be represented in the form

$$z_n' = \frac{F_n^2}{F_n^2 + G_n^2}\,, \tag{52}$$

where F_n and G_n are real quantities. In view of Eqn (52) and the equality $z_n''^2 = z_n' - z_n'^2$, we find that, in this case,

$$z_n'' = \pm \frac{F_n G_n}{F_n^2 + G_n^2} \,. \tag{53}$$

Since the quantities F and G have not yet been determined, the selection of a specific sign on the r.h.s. of Eqn (53) does not restrict the generality of the consideration. For certainty, let us select the minus sign. Then, putting everything together, we get

$$z_n = \frac{F_n^2}{F_n^2 + G_n^2} - \mathrm{i}\,\frac{F_n G_n}{F_n^2 + G_n^2} \equiv \frac{F_n}{F_n + \mathrm{i}G_n} \,, \tag{54}$$

where real F and G, of course, are functions of ε and R (actually, m and x).

What happens if finite dissipation is taken into account, i.e., if $\varepsilon = \varepsilon' + \mathrm{i}\varepsilon''$ and $\varepsilon'' \neq 0$? To answer this question, note that neither Maxwell's equations nor the corresponding boundary conditions contain terms in which ε would enter into a combination other than $\varepsilon' + \mathrm{i}\varepsilon''$. This means that the transition to the case of finite dissipation is reduced to the formal replacement of real ε by a complex one. This replacement makes the functions F and G complex, but does not change the structure of expression (54). Indeed, taking advantage of the known representation of the Hankel function, $H_\nu^{(1)}(z) \equiv J_\nu(z) + \mathrm{i}\,Y_\nu(z)$, where $Y_\nu(z)$ is the Neumann function [104], one can make sure that expressions (48), (49) perfectly agree with Eqn (54) at any complex value of ε. In this case, F_n are equal to the numerators of the r.h.s. of expressions (48), (49), and corresponding G_n are defined by the expressions

$$G_n^{\mathrm{sph}\,(a)} = \psi_n'(mx)\chi_n(x) - m\psi_n(mx)\chi_n'(x) \,, \tag{55}$$

$$G_n^{\mathrm{sph}\,(b)} = \psi_n(mx)\chi_n'(x) - m\psi_n'(mx)\chi_n(x) \,, \tag{56}$$

where $\chi_n(x) = -\sqrt{\pi x/2}\,Y_{n+1/2}(x)$.

Writing the scattering coefficients in the form of Eqn (54) makes it possible to draw an important conclusion about certain general properties of theirs. As noted in the main text of the review, the Mie resonances are defined by the condition $G_n = 0$. In this case, the corresponding scattering coefficient equals unity, and the partial scattering cross-section reaches its maximum. As shown above, in the absence of dissipation, all F_n and G_n are purely real. Then, expression (54) can be rewritten as follows: $z_n(\zeta) = (\mathrm{Re}\,\zeta)/\zeta$, where $\zeta \equiv F_n + \mathrm{i}G_n$.

Importantly, the function of the complex variable $z_n(\zeta)$ defined in this manner is not analytic at any point of the complex plane ζ. This is easy to verify, for example, by applying the Cauchy–Riemann conditions to it. If $z_n(\zeta)$ were an analytic function, then the following identity would have to be fulfilled under these conditions:

$$\frac{\partial z_n}{\partial F_n} + \mathrm{i}\,\frac{\partial z_n}{\partial G_n} \equiv 0 \,. \tag{57}$$

It is easy to see that, actually, the l.h.s. of expression (57) is $1/(F_n + \mathrm{i}G_n) \neq 0$ and the Cauchy–Riemann conditions are not met.

The point $\zeta = 0$ is a singular point of this function, in which it has no definite value — the value of $z_n(\zeta)$ at this point depends on the trajectories in the plane of ζ along which it is approached. Indeed, consider a set of paths $|G_n| = A|F_n|^\alpha$, where A and α are positive constants. It can be seen that, in this case, when $\zeta \to 0$, function $z_n \to 0$ at $0 < \alpha < 1$, and $z_n \to 1/(1 \pm \mathrm{i}A)$ at $\alpha = 1$, where the plus sign is taken if F_n and G_n have the same signs and minus if the signs are opposite. Finally, $z_n \to 1$ at $\alpha > 1$.

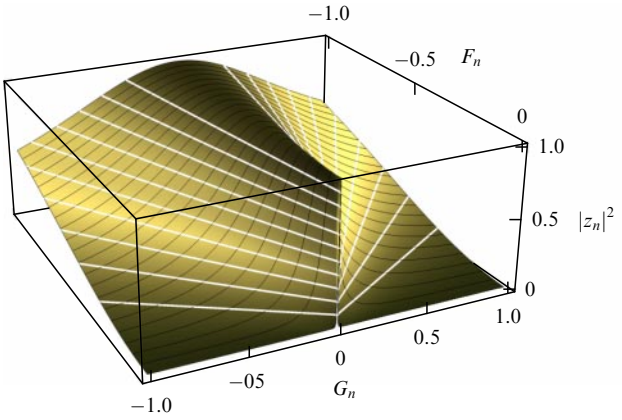

Figure 10. Surface $|z_n(F_n, G_n)|^2$ according to expression (54) with purely real F_n and G_n (nondissipative limit) and a set of lines $F_n = \mathrm{const}$ on it (thin black lines). The closer F_n to zero, the steeper the maximum of the lines at $G_n = 0$. Finally, the two wings of the surface intersect each other along line $F_n = G_n = 0$. Although different surface paths intersect this line at different values of $|z_n|^2$, all intersection points are projected onto the same point $F_n = G_n = 0$ in the plane (F_n, G_n). As an example of these trajectories, a set of $|z_n| = \mathrm{const}$ level lines for different constant values are shown by thick white lines [30].

To understand why such a simple function at first glance manifests such strange properties, consider the graph $|z_n|^2 = |z_n(\zeta)|^2$. This equality defines a surface in 3D space (see Fig. 10). It can be seen that two wings of this surface intersect each other along the line $\zeta = 0$. Although different trajectories lying on the surface $|z_n|^2 = |z_n(\zeta)|^2$ can cross this line at different values of $|z_n|^2$, all intersection points are projected onto the same point $\zeta = 0$ in the plane of the complex variable ζ, which explains the properties noted above. It is clear from the above consideration that this singularity is a generic property of the scattering coefficients. As shown below, it plays an important role in understanding various resonance effects of light scattering by subwavelength particles with low dissipation.

In particular, the dependence of the value of the scattering coefficients at the point $\zeta = 0$ on the trajectory along which this point is approached makes it fundamentally important to choose the correct trajectory. If all possible trajectories are equivalent in the mathematical sense, this is not the case in physics. Indeed, the natural physical set of independent variables is a pair R, ω. At the same time, the meaningful physical problem formulation is the study of scattering by a particle with a given value of R depending on the frequency of the incident radiation. As noted in the main text of the review, in this case the width of resonance lines decreases dramatically with a reduction in particle size. The accurate application of this approach removes the mathematical uncertainty in the values of the scattering coefficients at the point $\zeta = 0$. This issue is discussed in more detail in Ref. [30].

Consideration of small but finite dissipation shifts the values of the resonant frequencies (the solutions to the equation $G_n = 0$) from the real axis to the complex plane. As a result, G_n does not vanish at any real values of ω, and the singularity at $\zeta = 0$ disappears. In this case, at purely real ω,

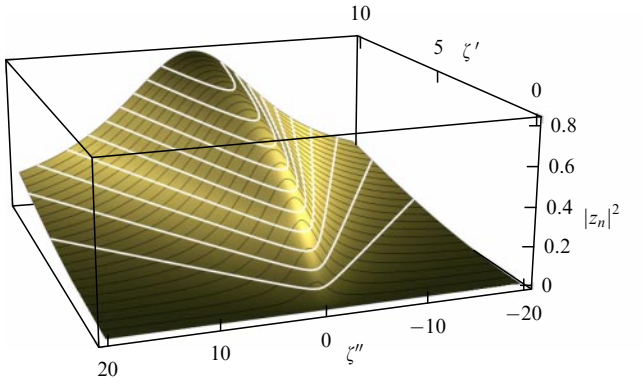

Figure 11. Same as in Fig. 10, but in the case of weak dissipation; see Eqn (58).

the function G_n becomes complex: $G_n = G_n' + \mathrm{i}G_n''$. At small dissipation ($|G_n'| \gg G_n''$), the profile $|z_n(\zeta)|^2$ becomes universal and, after the corresponding re-scaling of variables, similar to expression (17) reads as

$$|z_n|^2 \approx \frac{\zeta'^2}{(\zeta'+1)^2+\zeta''^2}, \quad \zeta = -\frac{F_n'}{G_n''} + \mathrm{i}\frac{G_n'}{G_n''} \tag{58}$$

(see Fig. 11). However, despite the removal of the singularity, everything said above regarding the resonant scattering in the vicinity of the point $R = 0$ remains valid with final dissipation too, at least as long as the radiative damping prevails over the dissipative one [30].

To end this discussion, note that the nonanalyticity of the scattering coefficients in the lossless case occurs only in the plane of complex ζ. If, instead, we consider the scattering coefficients as functions of a complex refractive index m or extend the real size parameter x to a complex plane, then, due to the representation of F_n and G_n in terms of the Bessel functions; see Eqns (48)–(50), (55), (56) and the analytic properties of the latter, all of them turn out to be analytic functions of m or x on the entire complex plane with the exception of the counting set of singular points.

References

1. Kerker M *The Scattering of Light and Other Electromagnetic Radiation* (Amsterdam: Elsevier Science, 2013)
2. Mie G *Ann. Physik* **25** 377 (1908)
3. Bohren C F, Huffman D R *Absorption and Scattering of Light by Small Particles* (Weinheim: Wiley-VCH Verlag, 1998)
4. Born M, Wolf E *Principles of Optics*: *Electromagnetic Theory of Propagation, Interference and Diffraction of Light* (Cambridge: Cambridge Univ. Press, 2013) § 13.5, https://doi.org/10.1017/CBO9781139644181; Translated into Russian: *Osnovy Optiki* (Moscow: Nauka, 1973) § 13.5
5. Eaton N *Vistas Astron.* **27** 111 (1984)
6. Krasnok A E et al. *Opt. Express* **20** 20599 (2012)
7. Chattaraj S, Madhukar A *J. Opt. Soc. Am. B* **33** 2414 (2016)
8. Chaâbani W et al. *ACS Nano* **13** 4199 (2019)
9. Staude I, Pertsch T, Kivshar Yu S *ACS Photon.* **6** 802 (2019)
10. Wriedt T *Part. Part. Syst. Charact.* **15** 67 (1998)
11. Kerker M *Aerosol Sci. Technol.* **1** 275 (1982)
12. Kelly K L et al. *J. Phys. Chem. B* **107** 668 (2003)
13. Wriedt T, in *The Mie Theory*: *Basics and Applications* (Springer Series in Optical Sciences, Vol. 169, Eds W Hergert, T Wriedt) (Berlin: Springer, 2012) pp. 53–71
14. Kuznetsov A I et al. *Science* **354** 6314 (2016)
15. Tzarouchis D, Sihvola A *Appl. Sci.* **8** 184 (2018)
16. Agranovich V, Gartstein Y *Metamaterials* **3** 1 (2009)
17. Merlin R *Proc. Natl. Acad. Sci. USA* **106** 1693 (2009)
18. Klimov V V *Nanoplasmonics* (Boca Raton, FL: CRC Press, 2013); *Nanoplazmonika* (Moscow: Fizmatlit, 2009)
19. Luk'yanchuk B et al. *Nat. Mater.* **9** 707 (2010)
20. Rahmani M *Small* **10** 576 (2013)
21. Strutt H J W *Philos. Mag.* **41** 274 (1871)
22. Strutt H J W *Philos. Mag.* **41** 447 (1871)
23. Landau L D, Lifshitz E M *Electrodynamics of Continuous Media* (Oxford: Pergamon Press, 1984); Translated from Russian: *Elektrodinamika Sploshnikh Sred* (Moscow: Nauka, 1982) § 8, § 80, § 84, § 92, § 105
24. Landau L D, Lifshitz E M *The Classical Theory of Fields* (Oxford: Pergamon Press, 1975) § 67; Translated from Russian: *Teoriya Polya* (Moscow: Fizmatlit, 2006) § 67
25. Landau L D, Lifshitz E M *Quantum Mechanics*: *Non-Relativistic Theory* (Oxford: Pergamon Press, 1977); Translated from Russian: *Kvantovaya Mekhanika. Nerelyativistskaya Teoriya* (Moscow: Nauka, 1989) Ch. XVII
26. Tribelsky M I *Europhys. Lett.* **104** 34002 (2013)
27. Bohren C F *Am. J. Phys.* **51** 323 (1983)
28. Tribel'skii M I *JETP* **59** 534 (1984); *Zh. Eksp. Teor. Fiz.* **86** 915 (1984)
29. Tribelsky M I, Luk'yanchuk B S *Phys. Rev. Lett.* **97** 263902 (2006)
30. Brynkin Ya A, Tribelsky M I *Phys. Rev. A* **100** 013834 (2019)
31. Tribelsky M I *Europhys. Lett.* **94** 14004 (2011)
32. Luk'yanchuk B S, Tribelsky M I "Anomal'noe rasseyanie sveta malymi chastitsami i obratnaya ierarkhiya opticheskikh rezonansov" ("Anomalous scattering of light by small particles and the inverted hierarchy of optical resonances"), in *Pamyati M.N. Libensona. Sbornik Vospominanii i Statei* (Memories of N.M. Libenson. Collection of Memoirs and Articles) (Eds D I Raskin, E B Yakovlev, G D Shandybina) (St. Petersburg: GU ITMO, 2005) pp. 101–117
33. Wang Z B et al. *Phys. Rev. B* **70** 035418 (2004)
34. Bashevoy M, Fedotov V, Zheludev N *Opt. Express* **13** 8372 (2005)
35. Luk'yanchuk B et al., in *2008 IEEE PhotonicsGlobal@ Singapore* (Piscataway, NJ: IEEE, 2008) p. 14
36. Tribelsky M I, Luk'yanchuk B S, in *Fundamentals of Laser-Assisted Micro- and Nanotechnologies* (Berlin: Springer, 2014) pp. 125–146
37. Svyakhovskiy S E, Ternovski V V, Tribelsky M I *Opt. Express* **27** 23894 (2019)
38. Tribelsky M I, Miroshnichenko A E *Phys. Rev. A* **100** 053824 (2019)
39. Canós Valero A et al. *Laser Photonics Rev.* **15** 2100114 (2021)
40. Chen S-W, Li J-H *Opt. Express* **25** 8950 (2017)
41. Shore R A *IEEE Antennas Propag. Mag.* **57** 69 (2015)
42. Garg S, Venkatapathi M *J. Opt.* **19** 075603 (2017)
43. Hasegawa K, Rohde C, Deutsch M *Opt. Lett.* **31** 1136 (2006)
44. Li R et al. *Nanotechnology* **26** 505201 (2015)
45. Fleury R, Soric J, Alù A *Phys. Rev. B* **89** 045122 (2014)
46. Ruan Z, Fan S *Phys. Rev. Lett.* **105** 013901 (2010)
47. Luk'yanchuk B S, Tribel'sky M I, Ternovsky V V *J. Opt. Technol.* **73** 371 (2006); *Opt. Zh.* **73** (6) 7 (2006)
48. Luk'yanchuk B et al. *J. Opt. A* **9** S294 (2007)
49. Lukyanchuk B et al. *J. Phys. Conf. Ser.* Vol. 59 (IOP Publishing, 2007) p. 234
50. Herlofson N *Arkiv Fysik* **3** 247 (1951)
51. Kaiser T R, Closs R L *Lond. Edinb. Dublin Philos. Mag. J. Sci.* **43** 1 (1952)
52. Closs R L, Clegg J A, Kaiser T R *Lond. Edinb. Dublin Philos. Mag. J. Sci.* **44** 313 (1953)
53. Baffou G, Quidant R, Garcia de Abajo F J *ACS Nano* **4** 709 (2010)
54. Skirtach A G et al. *Nano Lett.* **5** 1371 (2005)
55. Han G et al. *NanoBiotechnology* **3** 40 (2007)
56. Brigger I, Dubernet C, Couvreur P *Adv. Drug Deliv. Rev.* **54** 631 (2002)
57. Huang X et al. *Lasers Med. Sci.* **23** 217 (2007)
58. Anderson R, Parrish J *Science* **220** 524 (1983)
59. Pan L, Bogy D B *Nat. Photon.* **3** 189 (2009)
60. Luk'yanchuk B S et al. *New J. Phys.* **14** 093022 (2012)
61. Tribelsky M I et al. *Phys. Rev. X* **1** 021024 (2011)
62. Tribelsky M I, Fukumoto Y *Biomed. Opt. Express* **7** 2781 (2016)
63. Kraus J D, Marhefka R J *Antennas for All Applications* (New York: McGraw-Hill, 2002)

64. Balanis C A *Antenna Theory*: *Analysis and Design* (Hoboken, NJ: Wiley, 2016)
65. Miroshnichenko A E, Tribelsky M I *Phys. Rev. Lett.* **120** 033902 (2018)
66. Miller O D et al. *Opt. Express* **24** 3329 (2016)
67. Ruan Z, Fan S *Phys. Rev. A* **85** 043828 (2012)
68. Tretyakov S *Plasmonics* **9** 935 (2014)
69. Palik E (Ed.) *Handbook of Optical Constants of Solids* (San Diego: Academic Press, 1998)
70. Wood R W *Proc. Phys. Soc. Lond.* **18** 269 (1902)
71. Strutt J W *Proc. R. Soc. Lond. A* **79** 399 (1907)
72. Beutler H *Z. Phys.* **93** 177 (1935)
73. Fano U *Nuovo Cimento* **12** 154 (1935); cond-mat/0502210
74. Fano U *Phys. Rev.* **124** 1866 (1961)
75. Fano U *Current Contents* **27** 8 (1977)
76. Clark C W, in *A Century of Excellence in Measurements, Standards, and Technology* (Ed. D R Lide) (Boca Raton, Fl.: CRC Press, 2001) pp. 116–119; https://nvlpubs.nist.gov/nistpubs/sp958-lide/116-119.pdf
77. Berry R S, Inokuti M, Rau A R P *Biographical Memoirs Fellows R. Soc.* **58** 55 (2012)
78. Miroshnichenko A E, Flach S, Kivshar Yu S *Rev. Mod. Phys.* **82** 2257 (2010)
79. Tribelsky M I, Miroshnichenko A E, Kivshar Yu S *Europhys. Lett.* **97** 44005 (2012)
80. Zel'dovich Ia B *Sov. Phys. JETP* **6** 1184 (1958); *Zh. Eksp. Teor. Fiz.* **33** 1531 (1958)
81. Miroshnichenko A E et al. *Nat. Commun.* **6** 8069 (2015)
82. Ospanova A K, Stenishchev I V, Basharin A A *Laser Photon. Rev.* **12** 1800005 (2018)
83. Yang Y, Bozhevolnyi S I *Nanotechnology* **30** 204001 (2019)
84. Zurita-Sánchez J R *Phys. Rev. Res.* **1** 033064 (2019)
85. Savinov V et al. *Commun. Phys.* **2** 69 (2019)
86. Baryshnikova K V et al. *Adv. Opt. Mater.* **7** 1801350 (2019)
87. Gupta M, Singh R *Rev. Phys.* **5** 100040 (2020)
88. Li Y et al. *Nanophotonics* **9** 3575 (2020)
89. Ruppin R *Phys. Rev. B* **11** 2871 (1975)
90. Ruppin R *J. Opt. Soc. Am.* **71** 755 (1981)
91. Tribelsky M I et al. *Phys. Rev. Lett.* **100** 043903 (2008)
92. Miroshnichenko A E et al. *Opt. Photon. News* **19** (12) 48 (2008)
93. Tribelsky M I et al. *Phys. Rev. B* **94** 121110 (2016)
94. Mishchenko M *Light Scattering by Nonspherical Particles*: *Theory, Measurements, and Applications* (San Diego: Academic Press, 2000)
95. Papasimakis N et al. *Nat. Mater.* **15** 263 (2016)
96. Kildishev A V, Boltasseva A, Shalaev V M *Science* **339** 1232009 (2013)
97. Yu M, Capasso F *Nat. Mater.* **13** 139 (2014)
98. Cui T J et al. *Light Sci. Appl.* **3** e218 (2014)
99. Kabashin A V et al. *Adv. Funct. Mater.* **29** 1902692 (2019)
100. Feng T et al. *Phys. Rev. Appl.* **13** 021002 (2020)
101. Maheu B, Gouesbet G, Grehan G *J. Opt.* **19** 59 (1988)
102. Gouesbet G, Grehan G, Maheu B *J. Opt.* **19** 35 (1988)
103. Nieminen T A, Rubinsztein-Dunlop H, Heckenberg N R *J. Quant. Spectrosc. Radiat. Transf.* **79–80** 1005 (2003)
104. Abramowitz M, Stegun I A, Romer R H *Am. J. Phys.* **56** 958 (1988)